PHYSICAL REVIEW B VOLUME 28, NUMBER 11 1 DECEMBER 1983

Paramagnetic impurity effects in NMR determinations of hydrogen diffusion and electronic structure in metal hydrides. Gd^{3+} in YH_2 and $LaH_{2.25}$

T.-T. Phua, B. J. Beaudry, D. T. Peterson, and D. R. Torgeson
Ames Laboratory—U.S. Department of Energy and Department of Physics, and Department of Materials Science and Engineering, Iowa State University, Ames, Iowa 50011

R. G. Barnes
Ames Laboratory—U.S. Department of Energy and Department of Physics, Iowa State University, Ames, Iowa 50011 and Laboratory of Atomic and Solid State Physics and Materials Science Center, Cornell University, Ithaca, New York 14850

M. Belhoul, G. A. Styles, and E. F. W. Seymour
Physics Department, University of Warwick, Coventry CV4 7AL, England
(Received 6 June 1983)

Measurements are reported of the temperature dependence of the proton spin-lattice and spin-spin relaxation times T_1 and T_2 in yttrium and lanthanum dihydrides containing controlled levels of gadolinium as low as 50 ppm. The results demonstrate unambiguously that paramagnetic ions in concentrations so low as to have heretofore been regarded as insignificant have marked effects on the magnitude, frequency dependence, and temperature dependence of T_1 and to a lesser extent on T_2, and on the electronic structure and hydrogen diffusion parameters derived therefrom. The Gd^{3+} ion contributes an additional spin-lattice relaxation rate T_{1p}, which in these hydrides arises entirely from the dipolar coupling between impurity and proton moments. Proton magnetization is transported to the relaxation centers by spin diffusion at low temperatures and by hydrogen-atom diffusion at intermediate and high temperatures. The rate R_{1p} is directly proportional to Gd-ion concentration at both low and high temperatures, but in the atom diffusion regime R_{1p} is 20—25 times greater than for spin diffusion. The impurity-induced relaxation is shown to have profound effects on the apparent nuclear-nuclear dipolar relaxation rate R_{1d} associated with hydrogen diffusion. At impurity levels as low as 10 ppm Gd, a secondary minimum appears in the temperature dependence of T_1 which may be readily misinterpreted in terms of a second motional process with lower activation energy. Even lower impurity levels yield a characteristic "slope-change" effect, which may be construed as indicating a change in the activation energy for hydrogen diffusion. At low temperatures R_{1p} interferes with the determination of the conduction-electron contribution R_{1e} and the Korringa product $T_{1e}T$. Separation of R_{1e} and R_{1p} is complicated by the fact the R_{1p} is not temperature independent as has typically been assumed. Methods of achieving this separation are discussed, and it is shown experimentally that this difficulty can be circumvented by replacing the major part of the hydrogen with deuterium, thereby inhibiting spin diffusion. Measurement of T_1 as a function of resonance frequency and of T_2 can also be of value in separating the various sources of relaxation.

I. INTRODUCTION

Nuclear magnetic resonance (NMR) has been used for many years to investigate hydrogen locations, motion, and electronic structure in metal-hydrogen systems.[1-3] NMR is an effective technique for obtaining information about hydrogen motion since it is sensitive to the effects that such motion has on the proton spin-relaxation rates. These are functions of power spectra of the randomly varying nuclear dipole fields resulting from the atomic diffusive jumps. They depend on the strength of the dipolar interaction between protons (and in some cases with the metal nuclei as well), which depend in turn on the distribution of hydrogen among interstitial sites, and on the diffusive jump frequency. In particular, measurements of the proton spin-lattice relaxation time T_1 have been used to determine the activation energy of the diffusive motion and the temperature dependence of the hydrogen jump frequency. Information about electronic structure follows from the conduction-electron contribution to the spin-lattice relaxation rate $R_{1e}=(T_{1e})^{-1}$. The behavior of T_{1e} is governed by the well-known Korringa relation,[4] according to which $(T_{1e}T)^{-1/2}\propto N(E_F)$, where $N(E_F)$ is the density of states at the Fermi level. In the usual case where $N(E_F)$ is not appreciably temperature dependent, the generally assumed result, $T_{1e}T=$const, follows.

In most cases T_1 is measured as a function of temperature. A traditional schematic plot of the proton T_1 as a function of temperature in a metal hydride is shown in Fig. 1. The measured relaxation rate $R_1=(T_1)^{-1}$ is taken

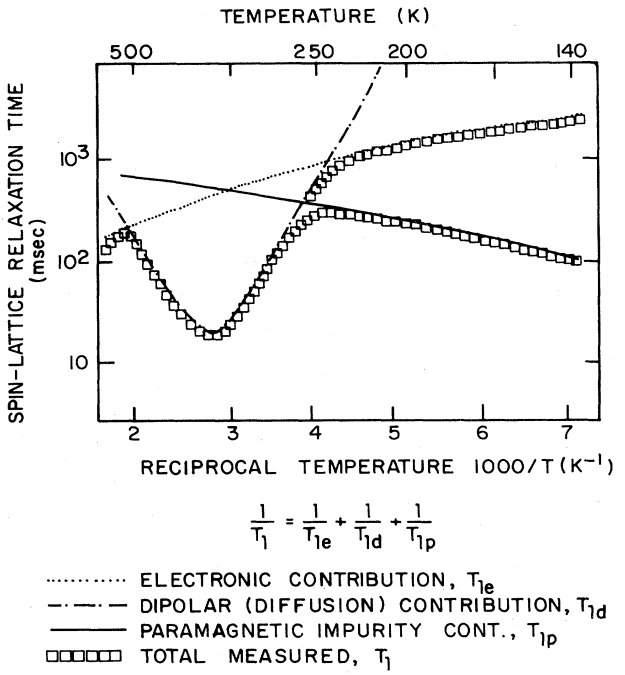

FIG. 1. Schematic plot of the logarithm of the proton spin-lattice relaxation time T_1 vs reciprocal temperature in a typical transition-metal hydride. The paramagnetic impurity contribution to T_1 is traditionally assumed to be most effective at low temperatures and less effective at high temperatures. The upper (lower) curve for $T<250$ K represents the resultant T_1 without (with) paramagnetic impurity.

to be the sum of the diffusion-controlled rate $R_{1d}=(T_{1d})^{-1}$ and the conduction-electron contribution R_{1e}, which is insensitive to hydrogen diffusion and should dominate at low and very high temperatures, outside the T_1 minimum region associated with the diffusion. In general, a contribution to R_1 from relaxation by paramagnetic impurities, $R_{1p}=(T_{1p})^{-1}$, may also be anticipated. The temperature dependence of T_{1p} has never been studied systematically for metal hydrides. The form of $T_{1p}(T)$ shown in Fig. 1 is that deduced by Schreiber and Cotts from their T_1 observations in lanthanum hydrides.[5] In many other cases, T_{1p} has been assumed to be temperature independent. In any event, the total spin-lattice relaxation rate may be written as

$$R_1=R_{1d}+R_{1e}+R_{1p} . \quad (1)$$

In a truly pure metal hydride, T_{1p} could be neglected, and at low temperature, for example, $R_{1d}\ll R_{1e}$, so that the measured $T_1=T_{1e}$. By using the Korringa relation, T_{1e} can be extended to higher temperatures and its contribution to the measured rate subtracted to yield T_{1d}. Information pertaining to the hydrogen jump frequency, activation energy, and diffusivity can be extracted from the dependence of T_{1d} on temperature by fitting some assumed spectral density function for the dipolar field fluctuations to the data.[3] In many cases in the literature, the actual impurity content of the samples studied has been unknown. Either they have been assumed to be sufficiently "pure" or some estimate of T_{1p} has been made, based on an assumption regarding the origin of the proton-impurity interaction and its temperature dependence. The principal purpose of the work reported here has been to delineate the range of effects associated with the presence of controlled levels of paramagnetic impurities in some typical metal-hydride systems.

It is well known that paramagnetic impurity ions play an important role in nuclear spin relaxation in insulating solids (e.g., ^{19}F in CaF_2) at low temperatures and at concentrations as low as 10—100 ppm.[6,7] Any excess energy in the nuclear spin system diffuses via the mutual nuclear spin-exchange process towards the much larger electronic magnetic moments of the impurity ions where relaxation occurs via direct dipolar coupling or transferred hyperfine interaction. These effects have also been studied in metallic hosts[8] where the coupling to the ions may be direct or through the conduction electrons [Ruderman-Kittel-Kasuya-Yosida (RKKY) interaction].

Impurity-induced relaxation effects are also known to occur at higher temperatures where translational motion of ions containing the resonant nuclei becomes important. The early work of Shen[9] on rare-earth impurities in LaF_3 and the recent discovery of "magnetic tagging" effects on Mn-doped PbF_2 by Jaccarino and co-workers[10] are illustrative. Since hydrogen in metal hydrides also moves very rapidly at readily accessible temperatures similar effects might be anticipated in the proton resonance. Indeed, at sufficiently high temperatures the situation can be expected to be strongly analogous to that for protons in aqueous solutions containing low levels of magnetic ions.[11]

Observations on $T_{1d}(T)$ in some hydrides have been found to conform to the theoretical expectations associated with a diffusion process that can be characterized by a single type of jump and a single activation energy. In such cases a plot of $\log T_{1d}$ versus reciprocal temperature has a symmetrical or almost symmetrical form[12] about the minimum as in Fig. 1. However, there exist in the hydride NMR literature many examples of considerably more asymmetric minima than the theories predict in the temperature dependence of the proton T_{1d}, with a shallower low-temperature slope interpreted as being due to a change to a diffusion mechanism with a lower activation energy (see, for example, Ref. 13). Secondary minima, perhaps only partially resolved, have also been observed on the low-temperature side of the minimum (as in Ref. 14, for example) and have been interpreted in terms of two coexisting but independent motions of the hydrogen. Moreover, the predicted proportionality of T_{1d} with the square of the resonance frequency at temperatures well below the minimum is not always observed. A partial listing of cases where the simple theory fails has been given by Jones.[15] All of these observations have prompted theorists to develop more sophisticated models to match the experimental findings, and in order to uncover the details of the different diffusion mechanisms. However, confusion and some loss of confidence in the NMR

method have also been the result of these complex observations. It will be our contention that low levels of paramagnetic impurities produce precisely these types of effects.

In the work reported here we have embarked on an entirely new series of measurements on two hydride systems, using starting materials with controlled impurity content. This work forms part of a comprehensive NMR study of hydrogen site occupancies, electronic structures, and diffusion in the hydrides of the group-III*B* metals Sc, Y, La, Lu, and other rare-earth elements.[16–22] Results of NMR investigations of the scandium and lutetium systems are planned to be reported elsewhere, as will further work on the La, Ce, Pr, and Nd dihydride and trihydride phases. In particular, work on the lanthanum trihydride phase LaH_x ($2.5 \leq x \leq 3.0$) has not been included in this report. There the complexities resulting from superlattice orderings and structural and electronic phase transitions[17,19,21] tend to obscure the character of the effects due to paramagnetic impurities, which are the principal subject of this paper.

Both yttrium and lanthanum react with hydrogen to form nonstoichiometric hydrides with a maximum [hydrogen]/[metal] ratio of 3.[23] The β-phase lanthanum hydride LaH_x exists from $x \gtrsim 1.9$ to $x=3$ and is fcc with a structure based on that of CaF_2 throughout this range at temperatures that are not too low. However, for $T \lesssim 270$ K, tetragonal superlattice ordering of the hydrogen occurs for $2.3 \lesssim x \lesssim 2.6$ (Refs. 17 and 19), and a tetragonal distortion of the metal lattice occurs[24] for $2.6 \lesssim x \lesssim 2.8$. For $x \lesssim 1.9$ the β phase coexists with the α-phase solid solution. For yttrium hydride YH_x, the cubic β phase exists only over the approximate composition range $1.8 \lesssim x \lesssim 2.05$ in the temperature range of interest (77–800 K).[23] At lower hydrogen concentrations coexistence of the α and β phases occurs. At the other extreme, the structure of yttrium hydride changes from cubic to hexagonal (HoD_3) as the trihydride composition is approached. Both the cubic and hexagonal phases exist in the range $2.05 \lesssim x \lesssim 2.8$, the hexagonal trihydride probably occurring as a single phase at concentrations $x \gtrsim 2.8$.

The yttrium and lanthanum hydrides studied in this investigation are all β-phase materials with the metal atoms located on an fcc lattice, as shown in Fig. 2. Hydrogen occupies predominantly the interstitial sites with tetrahedral symmetry (*T* sites), which form a simple cubic lattice with lattice parameter one-half that of the metal. A second type of interstitial site exists with octahedral symmetry (*O* sites) but lies higher in energy and so is not filled first. However, the premature occupancy of some *O* sites before all *T* sites have been filled has been detected by both NMR (Ref. 18) and neutron scattering[25] techniques in YH_2 and by NMR in LaH_2.[5]

The main objective of this investigation has been to study the effects of paramagnetic impurities on proton spin-lattice and spin-spin relaxation in the yttrium and lanthanum dihydrides. Accordingly, hydride samples were prepared from yttrium and lanthanum metals of several degrees of high purity and also from the metals containing controlled concentrations of rare-earth impurities that dissolve substitutionally in both metals. These dopants included Ce, Pr, Nd, Gd, Dy, and Er in quantities ranging from 50 to 1000 ppm (nominal) and in one case 10 000 ppm. A total of some 40 samples were studied, mainly through the temperature dependence of the proton T_1, with a less extensive study of the proton spin-spin relaxation time T_2. The temperature range covered was usually 77–800 K with some measurements extending to above 1250 K.

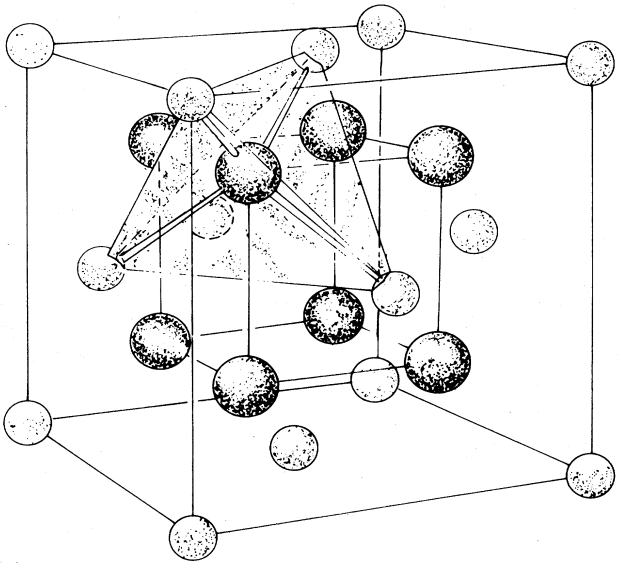

FIG. 2. Location of interstitial sites in fcc metal dihydrides. The small light spheres are metal atoms in fcc positions, and the larger dark spheres are hydrogen in tetrahedral sites. The tetrahedron formed by the four nearest-neighbor metal atoms is shown for one such hydrogen. The octahedral sites (not shown) are located midway between every pair of next-nearest-neighbor (NNN) metal atoms; they form a fcc lattice.

The results of these measurements and their interpretation are presented in two parts. In this paper we consider results for the *S*-state ion Gd^{3+}, since these are the most extensive and detailed. We present the results of a survey of the effects of controlled levels of both light and heavy rare-earth elements in YH_2 and to a lesser extent in $LaH_{2.25}$.[26] In this paper the theoretical background relating to proton relaxation processes is first reviewed. Following details of the experimental procedures and experimental results, an interpretation of the impurity-induced relaxation rates is given. Finally, the possibility of misinterpretation of these and similar data in terms of motions on two sublattices is pointed out, and the difficulties involved in determination of Korringa products are considered.

II. THEORETICAL BACKGROUND

In analyzing the experimental relaxation rates of the doped samples we shall assume that Eq. (1) is valid. It is then possible to determine the impurity-induced relaxation

rate R_{1p} by subtracting the measured rate R_1 of the pure sample from the measured rates of the impurity-doped samples. In so doing it is implicitly assumed that the conduction-electron contribution R_{1e} and the diffusion-controlled (nuclear dipole-dipole) contribution R_{1d} are intrinsic properties of the hydride that are unaffected by the low levels of impurities introduced. (Because of the difficulty in preparing doped and undoped samples with exactly the same hydrogen content, it sometimes was found preferable to use the difference between relaxation rates for samples with different levels of the same dopant where such samples turned out to have more precisely equal hydrogen concentrations. This is possible since we found throughout that R_{1p} is proportional to dopant concentration.) Since even the purest sample of $YH_{1.98}$, for example, still contains a total residual rare-earth element content of about 10 ppm and that of $LaH_{2.25}$ about 5 ppm as determined by mass spectrometric analyses, the question as to what are the "true" intrinsic parameters characterizing T_{1e} and T_{1d} requires careful attention. This point will become evident when the T_1 data are examined.

A. Dipolar and conduction-electron contributions

In order to understand T_{1p} it is necessary to know the diffusion parameters, which we obtain from the NMR data for the purest specimens, corrected where necessary for the effects of residual impurities. For T_{1d} we consider it sufficient to employ an exponential correlation function [Bloembergen-Purcell-Pound (BPP) function[27]] for the dipolar field fluctuations, so that we have, for relaxation by proton-proton dipolar coupling,

$$R_{1d}=\tfrac{3}{10}\gamma_n^4\hbar^2\left[\frac{\tau_c}{1+\omega_0^2\tau_c^2}+\frac{4\tau_c}{1+4\omega_0^2\tau_c^2}\right]\sum_i r_i^{-6}\,, \qquad (2)$$

where γ_n is the proton gyromagnetic ratio, $\hbar$ is Planck's constant, ω_0 is the proton resonance frequency, and τ_c is the correlation time, which for proton-proton dipolar interactions is $\tau_D/2$ where τ_D is the mean dwell time for the hydrogen motion. The sum is taken over all occupied interstitial sites; r_i is the distance of the ith site from a proton site taken as origin. A more sophisticated model is not warranted in view of the complications we mention shortly, and moreover, the conclusions about hydrogen diffusion in these dihydrides that we shall reach on the basis of Eq. (2) are of a sufficiently general nature not to be influenced by the simplicity of the model. Equation (2) neglects the contribution to R_{1d} from the stationary metal nuclei. Although this could readily be taken into account,[27] Eq. (2) is an excellent approximation for YH_2 in view of the very small magnetic moment of ^{89}Y (roughly 5% that of the proton). For the lanthanum hydrides, however, the neglect of the ^{139}La contribution causes about a 10% error in estimating τ_D from Eq. (2), which is not generally significant for the purpose at hand. (However, we shall need to consider the effect of ^{139}La-^1H dipolar interactions when we discuss the effects of partial deuteration later.) Equation (2) also assumes that τ_c is the same for all sites. For the purpose of analyzing T_{1p} for YH_2 we shall not need to become involved with the additional complexity arising from the occupation of some O sites, and we shall implicitly assume that only T sites are occupied. Further, we shall take τ_D to be the same for sites that are near neighbors to an impurity as for remote sites. We comment further on this point later. As usual, the time τ_D is assumed to result from a thermally activated process and is expressed as

$$\tau_D=\tau_0\exp[E_{\rm act}/(k_BT)]\,, \qquad (3)$$

where $E_{\rm act}$ is the activation energy, k_B is Boltzmann's constant, τ_0 is a constant prefactor related to the reciprocal of the jump attempt frequency, and T is the absolute temperature.

For the sake of simplicity we suppose that T_{1e} follows Korringa behavior, i.e., $T_{1e}T=K$, where K is temperature independent. We shall not attempt here to draw any detailed conclusions regarding band structure and density of states from the $T_{1e}T$ values.

B. Paramagnetic ion contribution

In general, the protons are coupled to the paramagnetic ions both by direct dipole-dipole interactions and indirectly through the conduction electrons (the RKKY interaction). Although the latter type of interaction between the ions themselves is important in determining their cooperative magnetic properties, it is less significant between ions and protons because of the small hyperfine interaction between protons and conduction electrons. Nevertheless, it is responsible for the Curie-Weiss-like proton Knight shifts observed in samarium and neodymium dihydrides[28] in the paramagnetic region, and also the hyperfine field of about 2 kG observed directly by zero-field proton NMR in the ferromagnetic phase of NdH_2 at about 1 K. The dipolar interaction makes no contribution to this hyperfine field because of the site symmetry. The temperature of 1 K is sufficiently far below the Curie temperature (~ 10 K) that it relates to the saturation magnetization, and we may attribute a RKKY hyperfine field of approximately 500 G to each of the four nearest-neighbor (NN) Nd^{3+} ions. This is to be compared with the local dipolar field, due to the Nd^{3+} moment of $3.52\mu_0$, of approximately 2.8 kG. Although the RKKY field scales among the rare-earth elements as $(g-1)[J(J+1)]^{1/2}$ and the dipolar field as $g[J(J+1)]^{1/2}$, the dipolar field should be the larger in all cases. Since, further, it is only any anisotropic part of the RKKY interaction that can give rise to relaxation (due to the $S_zI_\pm$ term) in the most important region ($\omega_0\tau_i^*\sim 1$, where τ_i^* is the correlation time for the electron-nucleus interaction and is to be defined more fully later) for our observations, it appears that the dipolar interaction will dominate in T_{1p}.

For relaxation via the fluctuations of the dipolar field of the impurity ion, we first follow the formulation of Rorschach,[29] appropriate to the rigid-lattice regime, i.e., temperatures sufficiently low that atomic diffusion can be ignored. A quantity C is introduced, which measures the interaction strength between an ion and a nucleus and which is defined by

$$\tau^{-1}(r)=Cr^{-6}\ , \tag{4}$$

where $\tau^{-1}(r)$ is the relaxation rate a single nucleus would have if held fixed at the distance r from the ion. For a powder sample C is given by[30]

$$C=\tfrac{2}{5}\gamma_p^2\gamma_n^2\hbar^2 J(J+1)\left[\frac{\tau_i}{1+\omega_0^2\tau_i^2}+\frac{7\tau_i}{3(1+\omega_e^2\tau_i^2)}\right], \tag{5}$$

where J, γ_p, τ_i, and ω_e are the angular momentum, gyromagnetic ratio, spin-lattice relaxation time, and Larmor frequency of the ion, respectively. In the final term within the large parentheses, ω_e^2 has been written for $(\omega_e\pm\omega_0)^2$ since clearly $\omega_e\gg\omega_0$. Moreover, in this term only, τ_i is strictly the transverse relaxation time of the ion, but for the dilute solutions we consider it should be a good approximation to use the spin-lattice time τ_i. This term is often ignored but can be of some importance in the present case, where it appears that $\omega_e\tau_i$ is not necessarily very large compared with unity, especially at higher temperatures.

1. *Spin-diffusion regime*

In this low-temperature regime, relaxation is transported to protons far from the impurity ion (magnetization is transported to the ion) by the mechanism of spin diffusion, which is characterized by the spin-diffusion coefficient D_s. D_s was first estimated by Bloembergen[30] to be $D_s\approx a^2/(50T_2)$ for a simple cubic lattice, where T_2 is the rigid-lattice spin-spin relaxation time of the protons, which can be determined from the measured linewidth, for example, and a is the nearest-neighbor spacing of protons. Here, since we are assuming hydrogen to occupy T sites, $a=a_0/2$ where a_0 is the lattice parameter. Lowe and Gade[31] have considered the spin-diffusion process more rigorously and find $D_s\approx 0.15\gamma^2\hbar/a$ for a simple cubic lattice, which gives values about 3 times larger than Bloembergen's values. These results need appreciable modification when other nuclei with significant moments such as ^{139}La are present; D_s is reduced approximately in the ratio of the proton linewidth arising from proton-proton interaction to that arising from all nuclear interactions.[11] The relative importance of the direct relaxation rate, characterized by C, and the rate due to spin diffusion, characterized by D_s, can be described in terms of a distance β, defined by

$$\beta=(C/D_s)^{1/4} \tag{6}$$

and usually called the pseudopotential radius. β is the distance from the ion at which the two rates are equal.

Two additional length parameters also enter the theory. The first of these is the radius of the sphere of influence of a single impurity ion,

$$R=[3/(4\pi N)]^{1/3}\ , \tag{7}$$

where N is the number of impurity ions per unit volume. For the CaF_2 structure of the MH_2 hydrides, this can be written as

$$R=0.391a_0/c^{1/3}\ , \tag{8}$$

where c is the fractional impurity concentration. The final length parameter defines the barrier radius within which spin diffusion is inhibited because the static field of the impurity has shifted the Larmor frequencies of adjacent protons to such an extent that energy-conserving mutual spin flips can no longer occur. This barrier radius is conventionally defined by

$$b=(3\langle\mu_p\rangle/\mu_n)^{1/4}a\ , \tag{9}$$

where μ_n is the proton moment. The effective static component of the ion moment is $\langle\mu_p\rangle$ and is given by

$$\langle\mu_p\rangle=\gamma_p\hbar J\left[B^2(x)+\frac{\partial B}{\partial x}\frac{2}{\pi}\tan^{-1}\left[\frac{2\pi\tau_i}{T_2}\right]\right]^{1/2}, \tag{10}$$

where $B(x)$ is the Brillouin function in which $x=\gamma_p\hbar JH_0/k_BT$, and H_0 is the applied field. Equation (9) requires modification in a straightforward way if other nuclei besides protons contribute to the proton linewidth (as, for instance, ^{139}La), the barrier radius being reduced. Moreover, due to a second-order effect of the impurity itself,[32] some spin diffusion can occur within the radius b, but we estimate that in the present case (largely because of rather short τ_i values) this is a rather small effect; it is equivalent to a small reduction in the effective value of b. Because of these complications both in b and in D_s, and also because of our assumption that only T sites are occupied in YH_2, we shall not look for precise agreement between theory and experiment.

With these parameters defined, the proton spin-lattice relaxation rate due to spin diffusion to the impurity is given by[29]

$$R_{1p}=8\pi ND_s\beta\frac{\Gamma(\frac{3}{4})}{\Gamma(\frac{1}{4})}\frac{I_{3/4}(\delta)}{I_{-3/4}(\delta)} \tag{11}$$

in which $I_m(\delta)$ is the modified Bessel function. The parameter δ is defined by $\delta=\beta^2/2b^2$. The validity of Eq. (11) is subject to the constraint that $R\gg\beta$, b, which means that the impurity concentration, N or c, is low. Two limiting cases of Eq. (11) arise naturally from the dependence of the I_m on δ. These are the slow and fast spin-diffusion limits.

In the slow spin-diffusion limit, the bottleneck is the rate at which spins can diffuse to the impurity ion. This occurs for $\delta\gtrsim 2$, and hence for $\beta\gtrsim 2b$, and leads to the result

$$R_{1p}\approx\frac{8\pi}{3}ND_s\beta=\frac{8\pi}{3}NC^{1/4}D_s^{3/4} \tag{12}$$

which was originally derived by Khutsishvili[33] and de Gennes.[34] In this case, T_{1p} is independent of the barrier radius. Richards[35] has recently given an interesting "scaling argument" for the $NC^{1/4}D_s^{3/4}$ dependence in this limit. The $\frac{1}{4}$ power is characteristic of an interaction, here dipolar, which is proportional to r^{-6}.

In the fast spin-diffusion limit the bottleneck is the rate at which the impurity can equilibrate spins in its immediate neighborhood. This occurs for $\delta\lesssim 0.3$, or $\beta\lesssim 0.8b$, and leads to

$$R_{1p} \approx \frac{8\pi}{3} N D_s \beta \left[\frac{\beta^3}{2b^3} \right] = \frac{4\pi}{3} \frac{NC}{b^3} , \quad (13)$$

a result first given by Blumberg.[36] In this case, T_{1p} is independent of the spin-diffusion coefficient. The transition between the two limits is achieved smoothly by the changing ratio of the Bessel functions in Eq. (11).[29]

2. *Atomic diffusion regime*

The general expression for T_{1p} discussed above holds for the relaxation produced by dilute paramagnetic ions in the temperature range where atomic diffusion is negligible compared to spin diffusion. With increasing temperature, atomic diffusion becomes significant and reinforces the interaction between the ions and spins that are far away from the relaxation center. An exception occurs for the fast spin-diffusion limiting case when an additional diffusion rate is of no value in improving the overall relaxation efficiency. Shen[9] first suggested replacing D_s by the atomic diffusion coefficient D_a in the temperature range where $D_a > D_s$, or equivalently $\tau_D \lesssim T_2$, which also defines the nuclear dipolar motional-narrowing region. Shen proposed that the expression for the slow-diffusion limit in this higher temperature range be

$$R_{1p} \approx \frac{8\pi}{3} N D_a \beta' , \quad (14)$$

where now

$$D_a = D_0 \exp[-E_{\rm act}/(k_B T)] \quad (15)$$

and

$$\beta' = (C/D_a)^{1/4} . \quad (16)$$

Richards[37] showed that, for $D_a \gg D_s$, this replacement of spin diffusion by atomic diffusion could be extended to Rorschach's general result, Eq. (11), giving

$$R_{1p} = 8\pi N D_a \beta' \frac{\Gamma(\frac{3}{4})}{\Gamma(\frac{1}{4})} \frac{I_{3/4}(\delta_a)}{I_{-3/4}(\delta_a)} , \quad (17)$$

with

$$\delta_a = (\beta')^2/(2a_1^2) , \quad (18)$$

where the barrier radius b has been replaced by the distance of closest approach of a proton to the impurity, $a_1 = (\sqrt{3}/4)a_0$ in the present case, and the correlation time for the interaction is now $\tau_i^{*-1} = \tau_i^{-1} + \tau_D^{-1}$. Just as in the spin-diffusion regime there is a fast atomic diffusion limiting form, which is obtained from Eq. (13) by replacement of D_s by D_a, β by β', and b by a_1. This limit is appropriate to temperature sufficiently high so that $\tau_D \ll \tau(a_1)$ and is the well-known result that has been used for many years to describe the relaxation of nuclei in liquids due to dissolved paramagnetic ions. Richards also treated the case, important over a small, intermediate temperature range, where D_a and D_s are comparable.

We therefore have the following expectations. If, for $\tau_D \lesssim T_2$, a system is in the slow spin-diffusion regime, increasing temperature causes an increase in R_{1p} as atomic diffusion enhances the overall process, merging into the slow atomic diffusion region. With further increase of temperature the fast atomic diffusion region is reached in which R_{1p} eventually decreases again. For this case, therefore, R_{1p} passes through a maximum when $\tau_D \approx \tau(a_1)$. If, on the other hand, a system is in the fast spin-diffusion regime for $\tau_D \lesssim T_2$, atomic diffusion will only enhance R_{1p} and eventually produce a maximum if $\beta > a_1$ at the temperature where D_a becomes greater than D_s. If $\beta < a_1$ when this occurs with further increase of temperature the result merges into that for fast atomic diffusion and the maximum characteristic of the previous case does not occur. (Of course, there is still a temperature dependence associated with τ_i^* contained in C.)

3. *Spin-spin and rotating frame relaxation times*

The treatment for T_{2p}, the proton spin-spin relaxation time due to dipolar interaction with the impurities, follows closely that for T_{1p}, with the appropriate change in the form of C in Eq. (5).[11] It is straightforward to show that, for $\omega_e^2 \tau_i^{*2} \ll 1$, $T_{2p} = T_{1p}$. Moreover, T_{2p} and T_{1p} differ by only a trivial factor close to unity at all temperatures for which $\omega_0^2 \tau_i^{*2} \ll 1$, since, if this inequality is satisfied, the quantity in large parentheses in Eq. (5), which enters T_{1p}, reduces to

$$\tau_i^* + \frac{7\tau_i^*}{3(1+\omega_e^2 \tau_i^{*2})} ,$$

and the corresponding quantity entering T_{2p} is

$$\tfrac{7}{6}\tau_i^* + \frac{13\tau_i^*}{6(1+\omega_e^2 \tau_i^{*2})} .$$

Thus in the range $\omega_0^2 \tau_i^{*2} \ll 1 \ll \omega_e^2 \tau_i^{*2}$, T_{2p}/T_{1p} lies between $\frac{6}{7}$ (slow-diffusion limit) and $(\frac{6}{7})^{1/4}$ (fast-diffusion limit). The main point is that $T_{2p} \approx T_{1p}$ over a wider temperature range than that for which $T_{2d} = T_{1d}$, provided that the condition $\omega_0 \tau_i \approx 1$ is reached at a lower temperature than that for $\omega_0 \tau_D \approx 1$.

A similar relationship occurs for $(T_{1\rho})_p$, the rotating frame spin-lattice relaxation time due to the impurities. For instance, if $\omega_0^2 \tau_i^{*2} \ll 1 \ll \omega_e^2 \tau_i^{*2}$, we find $(T_{1\rho})_p / T_{1p} = (\frac{6}{7})^{1/4}$ in the slow atomic diffusion regime, and $(T_{1\rho})_p / T_{1p} \approx (\frac{6}{7})^{1/4} 2^{3/4} = 1.62$ in the slow spin-diffusion regime. The additional factor in the latter case arises because spin diffusion is only one-half as effective in $(T_{1\rho})_p$ as in T_{1p}.[38]

III. EXPERIMENTAL DETAILS

A. Sample preparation

All the hydrides investigated were prepared in the Materials Sciences Division of the Ames Laboratory from high-purity Ames Laboratory lanthanum, yttrium, and rare-earth metals. The starting pure metals were analyzed by spark-source mass spectroscopy, and the results of these analyses are summarized in the Appendix. They show that the various batches of Y and La typically con-

TABLE I. Yttrium hydrides $Y_{1-y}Gd_yH_x$ investigated in this study.

x=[H]/[Y]	Impurity	Concentration of dopant, y (ppm)	Y metal used (Ames Laboratory)
1.81	Mainly Gd[a]	20[b]	Y-12979-W
1.91	Mainly Gd[a]	20[b]	Y-12979-W
1.98	Mainly Gd[a]	20[b]	Y-12979-W
2.03	Mainly Gd[a]	20[b]	Y-12979-W
1.98	Partly Gd[a]	2[b]	Y-12381-B[c]
2.00	Gd	50	Y-12381-B
1.98	Gd	100	Y-12381-B
1.96	Gd	200	Y-12381-B
1.99	Gd	475	Y-12381-B
1.98	Gd	915	Y-12381-B

[a]Concentration not controlled.
[b]Spark-source mass-spectroscopic determination.
[c]Y-12381B also contains 4 ppm Tb, 2 ppm Ce, 4 ppm Pr.

tained very low levels of paramagnetic rare-earth impurities, on the order of 5—10 ppm total, before they were doped with controlled levels of Gd. These dopings were accomplished by first preparing a 1-at.% master alloy, which was then diluted by remelting with additional Y or La to give the lower solute levels (50—900 ppm). Misch metal trihydride served as a source of high-purity hydrogen. The hydriding procedures have been described in previous papers; a complete description is also given in Ref. 19. Finally, the samples were sealed in quartz tubes. The samples are listed in Tables I and II, which also include the identification numbers of the yttrium and lanthanum metal used in their preparation.

B. NMR instrumentation

At the Ames Laboratory, relaxation time measurements were made with a 40-MHz phase-coherent pulsed NMR spectrometer. The sample probe consists of a single self-supporting copper rf coil tuned with two independently tunable capacitors to precisely 50 Ω to match the characteristic impedance of the transmission lines.[39] The Q of the rf sample coil was set to 40 at room temperature. A digital pulse programmer[40] incorporating an autoincrement circuit[41] was used to generate the inversion recovery pulse sequences used in the measurements. Recovery of the spectrometer routinely occurred 6 μsec after a 90° pulse with a probe Q=40 and using a fast-recovery limiting amplifier.[42] Temperatures in the range 120—800 K were achieved using a cylindrical counter-flow nitrogen gas-blowing system[43] with copper-Constantan or plantinum-platinum-rhodium thermocouples and a current-feedback temperature controller.[43]

Spin-lattice relaxation times T_1 were measured using a magnetization inversion recovery sequence: 180° pulse, variable time delay, 90° pulse, and free-induction decay (FID). By incrementing the time between the 180° and 90° pulses, the FID data were collected with a Biomation model no. 610B waveform analyzer and passed to a Digital Equipment Corportion model no. LSI-11/03 microcomputer. Each FID was processed[44] by digitizing at 256 points. The first few (e.g., 8) "channels" were summed in the computer. Next, several (e.g., 128) channels were summed in a region of the FID where the baseline level had been reached. The weighted difference, representing the initial amplitude of the FID relative to the baseline, was then stored in memory. These data are insensitive to all sources of baseline drift slower than a few hundred microseconds. The series of such data points, typically 100, each corresponding to a unique value of the delay time between the 180° and 90° pulses, represents the inversion recovery of the proton spin magnetization. The recoveries

TABLE II. Lanthanum hydrides $La_{1-y}Gd_yH_x$ investigated in this study.

x=[H]/[Y]	Impurity	Concentration of dopant, y (ppm)	La metal used (Ames Laboratory)
2.27	Mainly Ce[a]	4[b]	La-8681
2.24	Gd	50	La-8681
2.26	Gd	100	La-8681
2.25	Gd	200	La-8681
2.24	Gd	500	La-8681

[a]Concentration not controlled.
[b]Spark-source mass-spectroscopic determination.

were analyzed by least-squares fitting of an exponential curve to the data points.

For the 40-MHz proton resonance, a Varian Associates model V-4012 electromagnet provided a field of 9395 G, and for corresponding fields for 60, 24, and 12.2 MHz a VA-3800 electromagnet was used. Although the field was stable within acceptable experimental limits, a deuteron magnetic resonance field stabilizer[45] was used to prevent any residual drift.

The measurements at 7 MHz were made with a modified Polaron spectrometer and digital pulse programmer[40] at the University of Warwick. The rf probe could be heated to ~1300 K in a water-cooled furnace or cooled to ~150 K using a liquid-nitrogen bubble pump system. T_1 measurements were made with the pulse sequence already described and T_2 measurements with a Carr-Purcell-Meiboom-Gill (CPMG) sequence with a pulse separation which was varied between 50 μsec and several milliseconds. The data were processed using a Nicolet 1170 signal averager and an Intertec Data Systems Superbrain II microcomputer.

IV. RESULTS

A. Yttrium dihydrides

1. Proton relaxation

To test the ideas discussed in Sec. II, two series of yttrium dihydride samples were investigated. The first of these was prepared from nominal "high-purity" yttrium (Ames Laboratory Y-12979-W) and comprised four samples having $x=[H]/[Y]=1.81$, 1.91, 1.98, and 2.03. This yttrium contained approximately 20 ppm Gd (and much smaller levels of other rare-earth elements) according to the mass-spectroscopic analysis (see the Appendix). The second series was prepared from the "purest" (i.e., least Gd, but with comparable levels of Tb, Ce, and Pr) yttrium available (Ames Laboratory Y-12381-B), alloyed with Ames Laboratory gadolinium, and comprised five samples of $YH_{1.98}$ having controlled Gd content of 50, 100, 200, 475, and 915 ppm. A sample of $YH_{1.98}$ was also prepared from this "purest" yttrium to serve as a basis for comparison.

These two sets of samples provide two cross sections of impurity-associated effects on proton T_1 and T_2: (1) The effect of a modest impurity level as hydrogen concentration is varied, and (2) the effect of large changes in impurity level at fixed hydrogen concentration. In the following, the results of T_1 and T_2 measurements on these two sets of samples are presented in sequence, beginning with the series of variable hydrogen concentration.

A composite plot of $\log T_1$ vs $10^3/T$ for the YH_x series at 40 MHz is shown in Fig. 3. Several features of these data merit comment. First, all of the curves exhibit a definite subsidiary minimum on the low-temperature side of the principal T_1 minimum. Second, the temperatures at which both the principal and secondary minima occur decrease with increasing hydrogen content. For the principal minimum this behavior shows at once that at constant temperature the hydrogen diffusion rate increases with increasing hydrogen concentration. Similar behavior was noted by Schreiber and Cotts[5] in the case of lanthanum hydrides. Third, the values of T_1 obtained here are

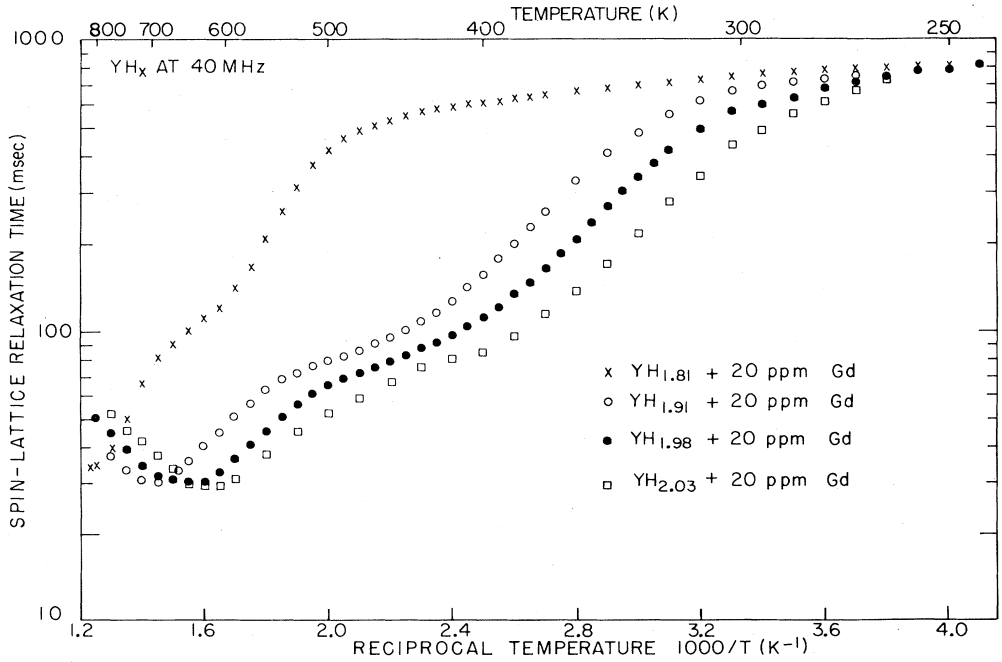

FIG. 3. A composite plot of $\log T_1$ vs $10^3/T$ for protons in a series of yttrium dihydrides with different hydrogen concentrations. The same yttrium metal, batch Y-12979-W, was used for all four samples.

much larger throughout the temperature range than those reported by Kashaev *et al.*,[14] consistent with the nominal high purity of the present samples and showing that considerable levels of paramagnetic impurity were present in the samples of Ref. 14. And fourth, although the depth of the principal minimum increases (i.e., R_1 increases), consistent with the increase in hydrogen concentration, the depth of the secondary minimum remains nearly constant. This result is surprising since if the secondary minimum reflects hydrogen motion on the *O*-site sublattice,[14] then the relative depths of the secondary and principal minima are related to the *O*-site occupancy (see Sec. VI). These results would then suggest that little change in *O*-site occupancy occurs over the dihydride composition range—a surprising and unlikely conclusion.

The proton T_1 values in the purest sample of $YH_{1.98}$ are much larger than those shown in Fig. 3 for the pure sample of $YH_{1.98}$ over the entire temperature range. For the purpose of direct comparison, the T_1 values at 40 MHz for the pure and purest samples are shown in Fig. 4. Not only are the low-temperature T_1 values larger for the latter, but the subsidiary minimum has essentially vanished. The principal difference between the two batches of yttrium metal used for these samples is the concentration of Gd, i.e., 2 ppm in the purest sample and 20 ppm in the pure sample, as determined by mass-spectroscopic analysis.

The most striking feature of the data is the disappearance of the subsidiary minimum for the purer sample. All that remains for that sample is a weak depression in the T_1 curve, which causes a change to a smaller slope in that temperature region. As previously remarked, this slope-change feature has been reported in other metal hydrides and has been attributed to a change in the activation energy for hydrogen diffusion. Such claims have to be investigated further; however, one can conclude without doubt that the subsidiary minimum seen in the YH_x samples of Fig. 3 is caused by the presence of $\sim$20 ppm Gd. Furthermore, the slope-change feature in the purest sample can surely be ascribed to the remaining 2 ppm Gd plus other impurities (mainly Pr and Tb). Therefore, it appears likely that only a single diffusion-induced minimum without slope change or other anomalies on the low-temperature side will be observed if an entirely impurity-free hydride can be obtained. This conclusion is confirmed by the analysis discussed in Sec. V. Since it is clear from other evidence[18,25] that there is substantial *O*-site occupancy, such a single minimum may imply that the times associated with jumps between various sites are not very different from one another, or that frequent jumps occur between sublattices, so that separate minima cannot be resolved.

It may be noted that the temperature of the principal T_1 minimum is shifted from 655 K for the pure sample to 690 K for the purest sample. This shift is thought to be due to a small difference in the true hydrogen concentrations, within the typical uncertainty of $\pm 2\%$ in their individual determinations.

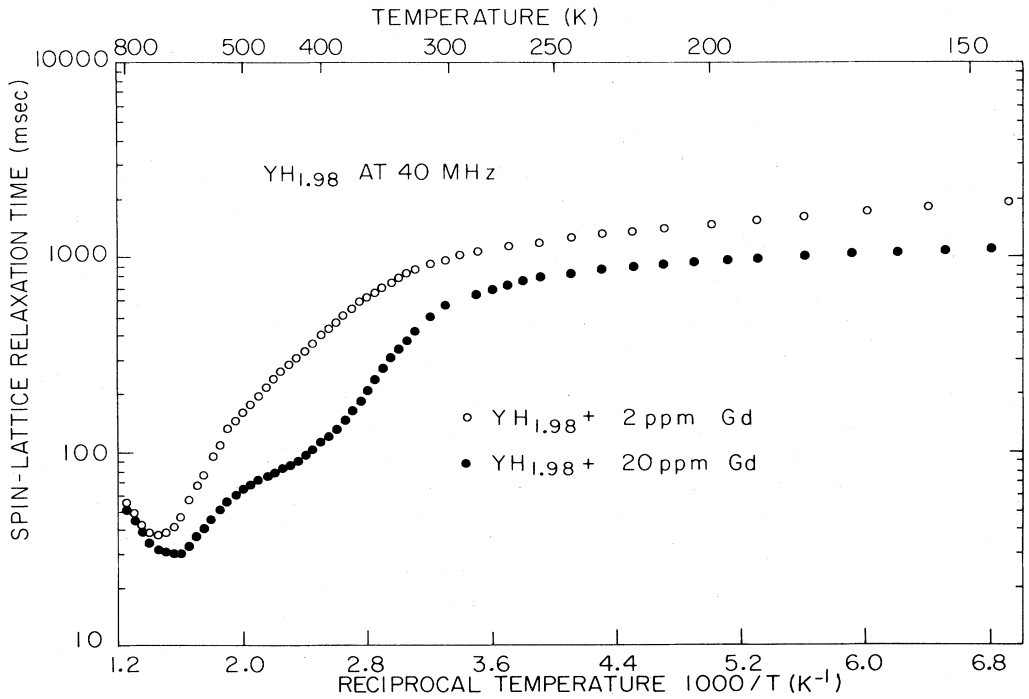

FIG. 4. Comparison of $\log T_1$-vs-$10^3/T$ plots of protons in $YH_{1.98}$ samples containing 2 ppm Gd and 20 ppm Gd (as determined by mass-spectroscopic analysis). The disappearance of the subsidiary minimum and the increase of T_1 at low temperatures are apparent in the data for the purer sample.

The T_1 values measured at 40 MHz in the series of $YH_{1.98}$ samples containing controlled levels of Gd, $Y_{1-x}Gd_xH_{1.98}$, are shown in Fig. 5. The data for both the purest and pure $YH_{1.98}$ samples have been included for comparison. Depression of T_1 by the Gd impurity is observed over the entire temperature range from 77 to 880 K. The depth of the subsidiary minimum increases with increasing Gd concentration, and the two minima merge into a single broad minimum as the concentration becomes greater than about 200 ppm. For the 915-ppm sample, the effect of the Gd addition is so overwhelming that no trace of the original principal minimum remains.

Even though the purest $YH_{1.98}$ sample still shows some residual effects from the approximately 10-ppm total impurity level, it is the purest yttrium hydride available in this study. The relaxation rate due to the Gd^{3+} ion-proton interaction, R_{1p}, can be determined with good accuracy by subtracting the rate for the purest sample from those of the Gd-doped samples. The resulting values of R_{1p} at 40 MHz are plotted in Fig. 6. For temperatures below 250 K, the rates for all samples show only weakly temperature-dependent behavior (this aspect is considered further in Sec. V). The rates increase rapidly for temperatures between 300 and 400 K and then reach a broad maximum at higher temperatures. Qualitatively, this resembles the "magnetic tagging" effect in Mn-doped PbF_2 reported recently by Vernon *et al.*[10] In the temperature range 300—400 K the slopes of the $\log(R_{1p})$-vs-$10^3/T$ curves are identical for all the samples. We shall see that this means that the activation energy for hydrogen diffusion is the same in all the samples, independent of Gd concentration.

Figure 7 shows a log-log plot of the relaxation rates at 40 MHz due to the impurity at 145 and 500 K as a function of Gd concentration. At both temperatures R_{1p} is directly proportional to Gd concentration within experimental error. However, the impurity-induced rate at 500 K is about 20 times stronger than that at 145 K. Thus the impurity ions are much more effective in relaxing proton spins at higher temperatures where the hydrogen is in rapid diffusive motion. In Fig. 7 the R_{1p} values for the pure sample (20 ppm Gd by mass spectroscopy) fall on the lines at an impurity concentration of 11 ppm. This is not inconsistent with the estimated accuracy of the mass spectroscopic analyses (a factor of about 2 at these impurity levels).

Since a knowledge of the frequency dependence can often be helpful in relaxation studies, we have measured T_1 at 200 K (as representative of the lower-temperature region) for the $YH_{1.99}$ + 475-ppm Gd sample at frequencies of 60, 40, 24, and 12.2 MHz, yielding values of 76.0, 59.5, 46.3, and 36.2 msec, respectively. This change must be attributed to a decrease of R_{1p} with increasing frequency, since corresponding results for pure samples showed

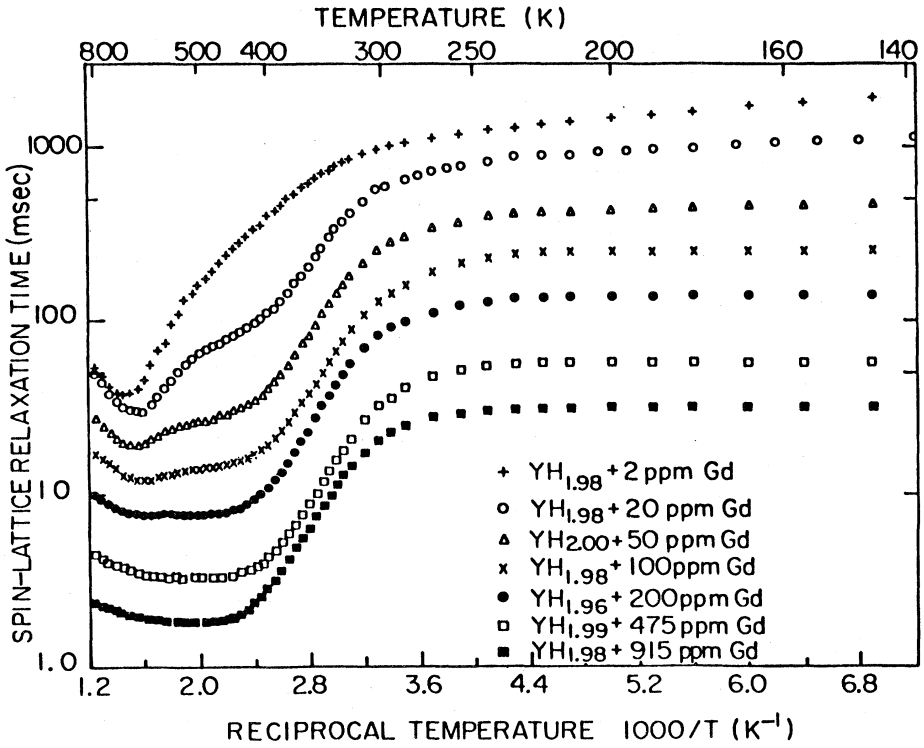

FIG. 5. Composite plot of $\log T_1$ vs $10^3/T$ at 40 MHz for protons in yttrium dihydrides containing various Gd concentrations. The Gd content in the two samples with the least impurity was determined by mass-spectroscopic analysis, whereas that in the other samples was controlled during preparation.

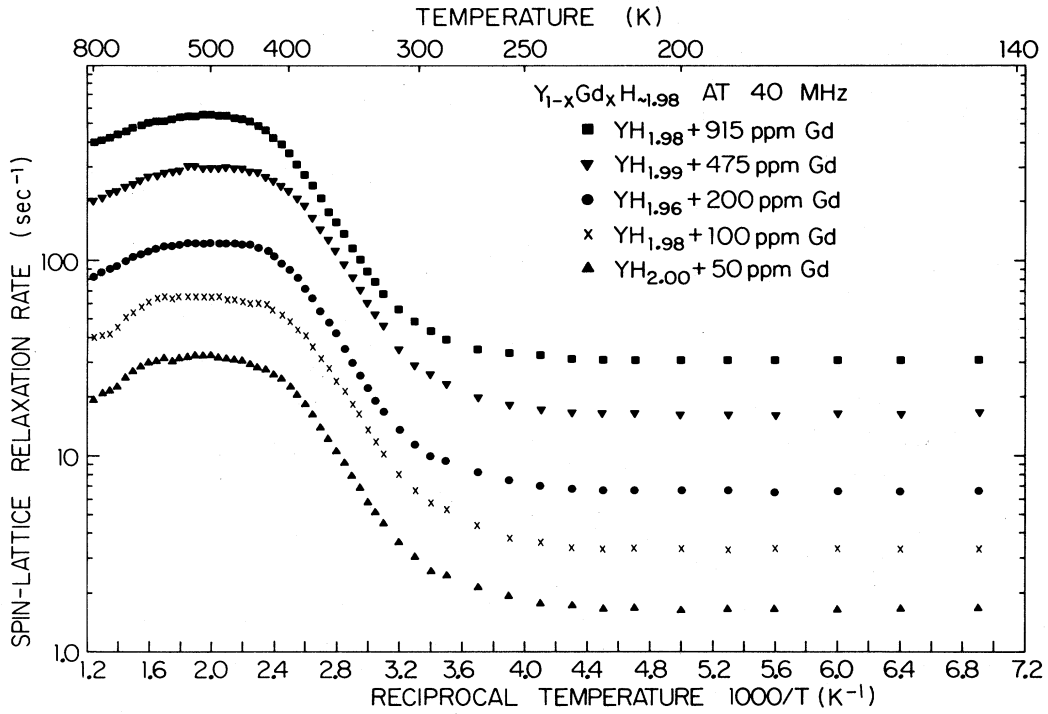

FIG. 6. Composite plot of $\log R_{1p}$ vs $10^3/T$ for the series of Gd-doped yttrium dihydride samples. R_{1p} is obtained from the data of Fig. 5 as explained in the text.

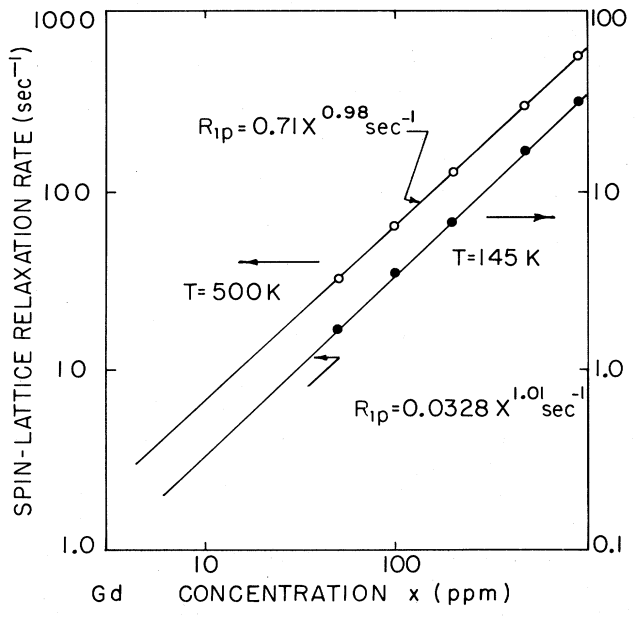

FIG. 7. $\log R_{1p}$ vs $\log x$ in $YH_{1.98}$ at $T=145$ K and at $T=500$ K measured at 40 MHz. The solid lines are least-squares fits. The $\log R_{1p}$ values for the sample for which mass-spectroscopic analysis indicated 20 ppm Gd would fall on the lines at a Gd concentration of 11 ppm.

very little frequency dependence. These observations will be discussed in Sec. V in connection with the Gd-ion spin-lattice relaxation time and the spin-diffusion barrier radius.

To obtain a measure of frequency dependence at higher temperatures we have measured T_1 for the group of samples to which Fig. 5 refers at 7 MHz and above room temperature (Fig. 8). The development of a subsidiary minimum at about 400 K is again shown. It is found that, as for the 40-MHz data, subtraction of rates again shows a broad maximum in R_{1p}. An example will be shown later (Fig. 17). For comparison purposes, Fig. 8 shows the behavior of the proton T_2 for the purest and the most heavily doped of the samples, and all the experimental T_2 data are collected in Fig. 9. It is striking that, in the temperature region around 400 K where T_1 is very sensitive to Gd content, the T_2 values are almost independent of Gd content; that is to say, the rate R_{2p} due to Gd is not detectable in the presence of the rapid, intrinsic R_2, whereas R_{1p} is a very clear contributor to R_1 in this temperature region. At temperatures above the main T_1 minima gadolinium does have an effect on T_2, and T_1 and T_2 become equal for each specimen. Above about 700 K, T_2 again falls below T_1. Also, above 1000 K, T_1 ceases to increase with increasing temperature in a manner which cannot be accounted for by a T_{1e} term (if $T_{1e}T$ is temperature independent). These effects are clearly not related to the presence of gadolinium and will be discussed elsewhere. We believe that these effects are related to

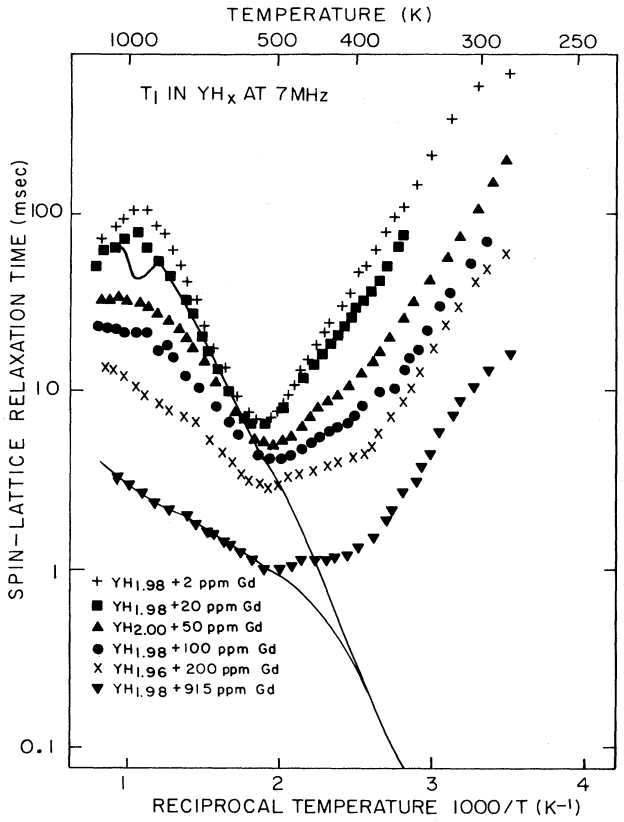

FIG. 8. Temperature dependence of the proton T_1 at 7 MHz for the specimens for which 40-MHz data are presented in Fig. 5. The symbols are the same as used in Fig. 9. The solid lines show, for comparison, the T_2 results for the two extremes of Gd concentration, taken from Fig. 9. Some of the experimental points around the minima for the purer samples have been omitted for clarity.

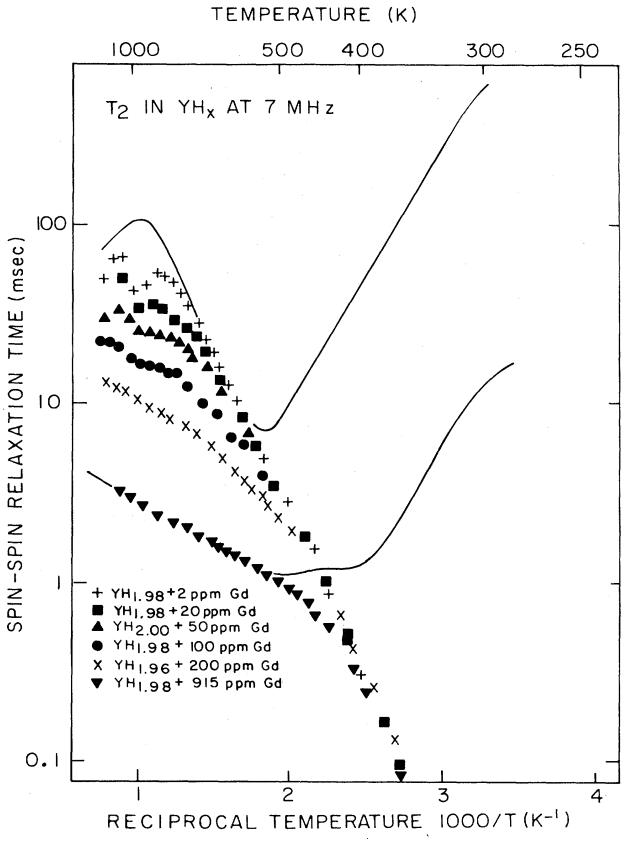

FIG. 9. Temperature dependence of the proton T_2 at 7 MHz (corresponding to the T_1 data of Fig. 8). The solid lines show for comparison the T_1 results for the two extremes of Gd concentration, taken from Fig. 8. Some of the experimental points in the overlap region have been omitted for clarity.

strong changes in the *O-T* distribution of the hydrogen ions.

2. *Deuteron relaxation*

Finally, the spin-lattice relaxation time of the ^2D nucleus in $YD_{1.88}$ has been measured at 7 MHz in the temperature range 269–670 K. The results are shown in Fig. 10, where it can be seen that T_1 goes through a symmetric minimum of $T_1=446$ msec at $T=411$ K. The aim of these measurements was originally to investigate the isotope effect in the diffusion of deuterium together with possible electric quadrupole relaxation processes. However, it is now clear that the sample contained an uncertain amount of Gd impurity probably comparable with that in the pure hydride samples, i.e., ~20 ppm. Consequently, as discussed in detail in Sec. V, we expect the effects of a paramagnetic contribution to the relaxation to be important and indeed probably strong enough to mask both isotope and quadrupole effects.

B. Lanthanum dihydrides

1. *Proton relaxation*

In order to determine that the effects of the Gd impurity described in Sec. IV A were not unique to the yttrium hydrides, a series of $LaH_{2.25}$ samples containing controlled levels of Gd was also studied. These samples were all prepared from lanthanum metal La-8681 and were doped with 50, 100, 200, or 500 ppm of Gd. The hydrogen concentration ([H]/[La]=2.25) was chosen in order that good coverage of the temperature region of the principal T_1 minimum due to hydrogen diffusion would be obtained at the resonance frequency of 40 MHz.

Qualitatively, the presence of Gd^{3+} has the same effects on the proton T_1 as in the yttrium hydrides. A depression of T_1 over the entire temperature range investigated is again observed. A composite plot of the T_1 results in this series is shown in Fig. 11. Features similar to those in $YH_{1.98}$ again appear: the growth in strength of the sub-

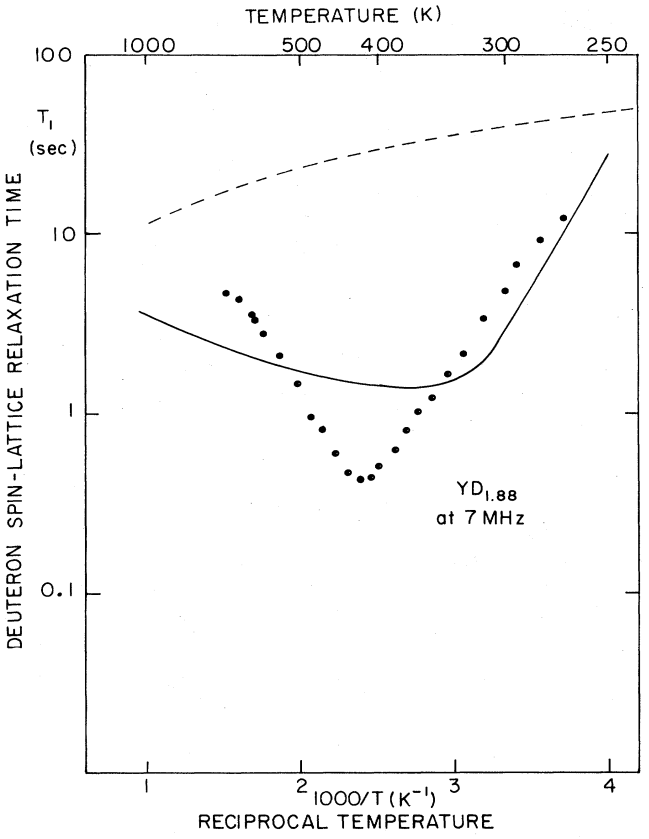

FIG. 10. Temperature dependence of the deuterium T_1 at 7 MHz in $YD_{1.88}$. For comparison the solid line shows the theoretical paramagnetic contribution calculated using Eq. (17) for a concentration of 20 ppm Gd, and the broken line shows T_{1e} as deduced from that in $YH_{1.92}$ allowing for the difference in the ^2D and ^1H gyromagnetic ratios.

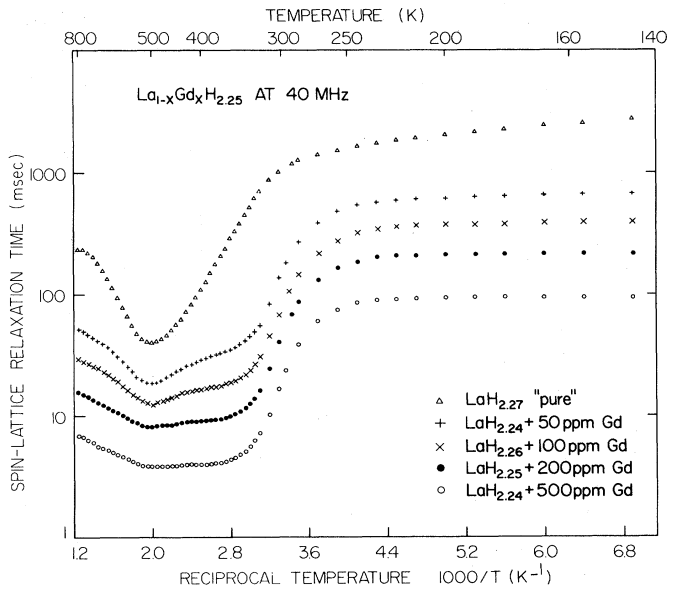

FIG. 11. Temperature dependence of the proton T_1 at 40 MHz in Gd-doped lanthanum dihydride $LaH_{2.25}$ for various Gd concentrations.

sidiary minimum with Gd concentration, the merging of the two minima at the highest Gd concentration, and the weakly temperature-dependent relaxation times at low temperatures. A single BPP function plus a Korringa term were used to fit the T_1 data for the pure $LaH_{2.27}$ sample. The result of this fit is shown in Fig. 12 and is seen to be extremely satisfactory, showing the expected behavior for an "impurity-free" hydride characterized by a single correlation time for the diffusional motion. In fact, the principal impurity in this metal is 4 ppm Ce, as determined by the mass-spectroscopic analysis. The best-fit parameters for Fig. 12 are the following: $E_{\rm act}=0.35$ eV/atom, $\tau_0^{-1}=7.4\times10^{11}$ sec^{-1}, $(T_1d)_{\rm min}=42.1$ msec, and $K=410$ sec K.

The procedure used to extract the impurity-induced relaxation rate R_{1p} in the $YH_{1.98}$ case was again applied, i.e., the measured relaxation rate R_1 for the pure sample of $LaH_{2.27}$ was subtracted from the other measured rates. The resulting values of R_{1p} are plotted in Fig. 13. The dependence of R_{1p} on Gd concentration is found to be the following: $R_{1p}=0.026x^{0.97}$ sec^{-1} at 145 K, and $R_{1p}=0.80x^{0.91}$ sec^{-1} at 500 K. Thus the rate is closely proportional to the Gd concentration and is about 25 times greater at high temperature than at low. At all temperatures Gd is rather less effective as a source of relaxation in $LaH_{2.25}$ than in $YH_{1.98}$.

2. *Effects of partial deuteration*

A further experiment was performed on a pair of partially deuterated samples, $La(H_{0.25}D_{0.75})_{2.25}$, both pure and doped with 90 ppm Gd. The 40-MHz proton T_1 data for these samples, together with the data for the corresponding undeuterated samples, are shown in Fig. 14. The rates

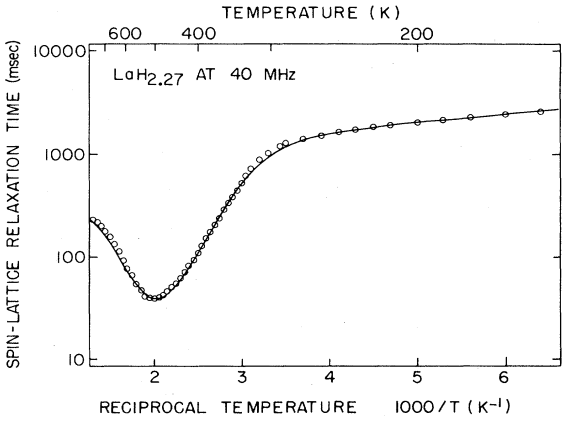

FIG. 12. Temperature dependence of the proton T_1 in the pure, undoped sample of $LaH_{2.27}$. The solid line is the least-squares best fit using a single BPP function and a temperature-independent Korringa constant. The fitting parameters are given in the text.

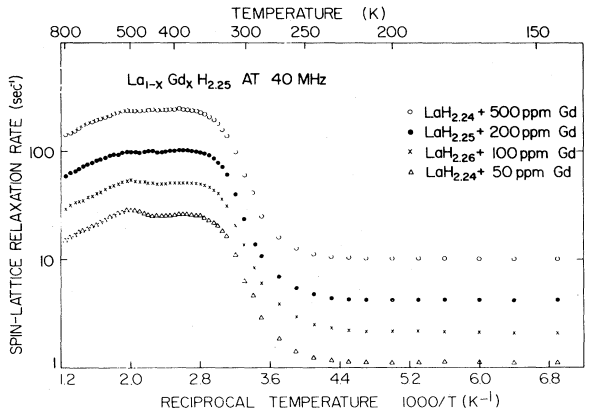

FIG. 13. Temperature dependence of the impurity-induced relaxation rate R_{1p} for the various Gd concentrations in $LaH_{2.25}$ at 40 MHz.

R_{1p} in the deuterated and undeuterated doped samples are shown in Fig. 15. As discussed in the next section, the equality of R_{1p} at high temperatures (after adjustment of the slightly different Gd levels) and the reduction of R_{1p} by deuteration at low temperatures provide a graphic demonstration of the changeover from an atomic-diffusion-dominated process to a spin-diffusion-dominated process.

C. ESR measurements

Finally, electron-spin-resonance (ESR) observations were made at 9.3 GHz of the Gd^{3+} resonance in the $YH_{1.98}$ + 915-ppm Gd and $LaH_{2.25}$ + 500-ppm Gd samples. In the former the linewidth was 615 G at 245 K and 225 G at 77 K. These widths correspond to relaxation times of 1.1 and 2.9×10^{-10} sec, respectively; they increase less rapidly than the proportionality with temperature that would arise from a Korringa process, and it is assumed that there is additionally a temperature-independent contribution. Allowance for this leaves $\tau_i T=3.7\times10^{-8}$ sec K. This value could be somewhat too small if there were a significant relaxation rate via phonons, which would be proportional to T^2 for $T\gtrsim\Theta_D/2$, i.e., $T\gtrsim100$ K. Since Gd^{3+} is a spin-only ion, such a term would be likely to be small and might only be important above room temperature. These results and conclusions are consistent with the results of Drulis[46] on 3 at.% Gd in $YH_{1.85}$, who observed somewhat smaller widths but generally increasing with increasing hydrogen concentration, and also increasing linearly with temperature.

For $LaH_{2.25}$ + 500 ppm Gd a very broad line ~900 G wide was observed at 77 K and no resonance was found at 295 K. It is therefore not possible to deduce a $\tau_i T$ value. Instead, we assume that $\tau_i T$ is not very different from that in $YH_{1.98}$ on the basis that $\tau_i/T_{1e}=(J_{sf}/A_{hf})^2$ if both τ_i and T_{1e} are Korringa-like, and that the Gd^{3+} conduction-electron exchange J_{sf} and proton—conduction-electron hyperfine coupling A_{hf} are unlikely to be very different for the two samples. Again, this is broadly consistent with Drulis's results.[46]

V. INTERPRETATION OF IMPURITY-INDUCED RELAXATION RATE

Since the effects of Gd in $YH_{1.98}$ and $LaH_{2.25}$ are so similar, the results will be considered in detail for the

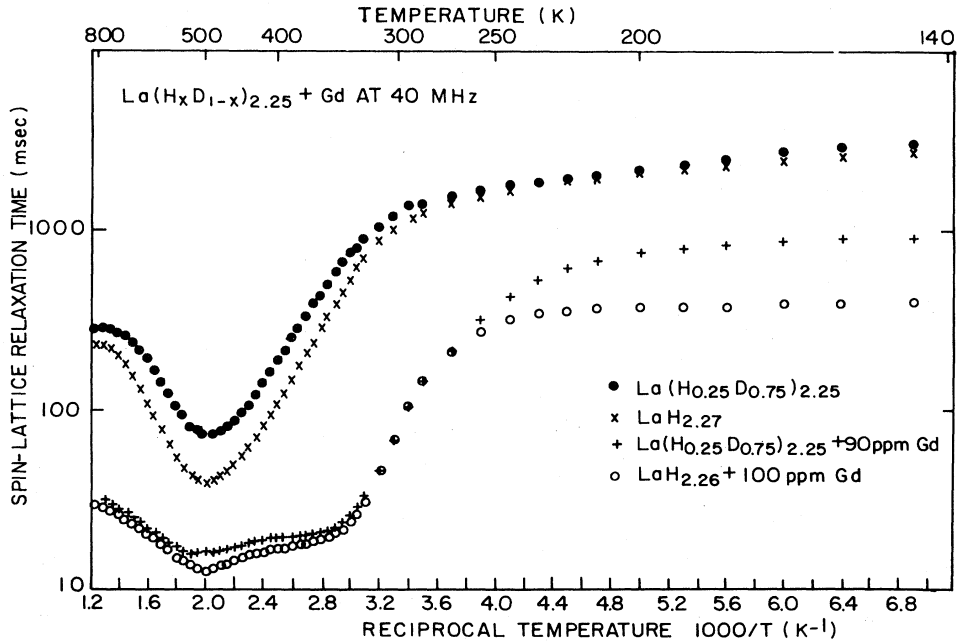

FIG. 14. Temperature dependence of the proton T_1 at 40 MHz in pure and Gd-doped lanthanum dihydride, compared with that for similar samples in which three-quarters of the hydrogen is replaced by deuterium.

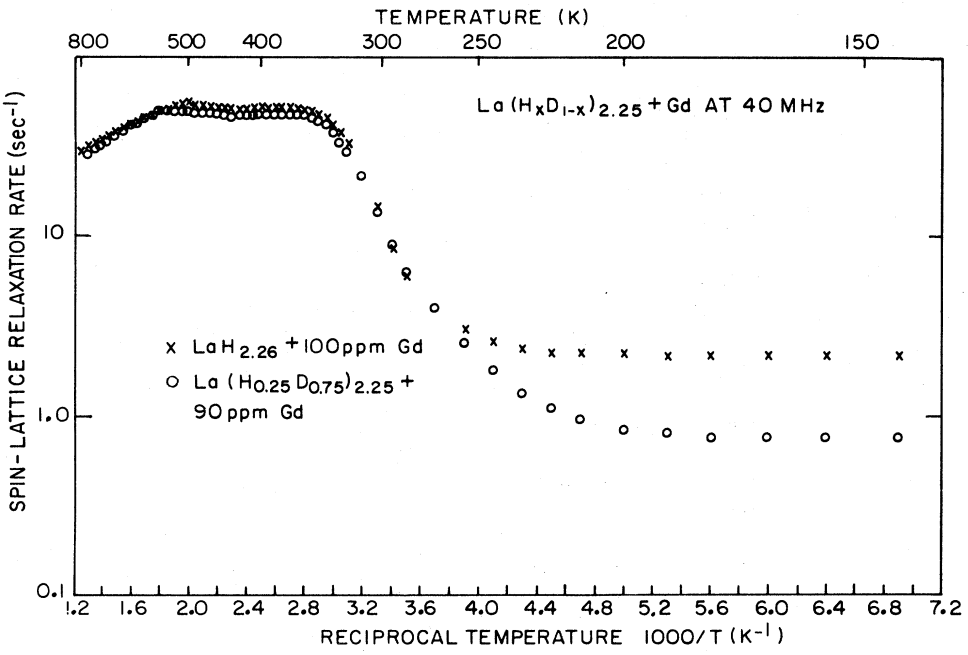

FIG. 15. Effect of partial deuteration on the temperature dependence of the Gd-induced relaxation rate $R_{1\rho}$ in lanthanum dihydride.

former and only points of difference noted for the latter. This choice is dictated both by the greater extent of the data for $YH_{1.98}$ and by the fact that the complication of O-site occupation is less severe. In one sense, however, the situation is more difficult in the $YH_{1.98}$ case: Whereas the undoped $LaH_{2.25}$ sample gave a $T_1(T)$ curve (Fig. 12) that was satisfactorily described without a residual $T_{1\rho}$ term, this is not so for even the purest $YH_{1.98}$ sample. Now although analysis of the data to give the diffusion parameters is not required to obtain values of $T_{1\rho}$, a knowledge of them is necessary in order to interpret $T_{1\rho}$ in terms of the theory of Sec. II. This was dealt with in the following manner. Since $R_{1\rho}$ due to Gd is known to be proportional to Gd concentration, allowance for the residual impurity (which is, most importantly, Gd) was made by subtracting from the observed R_1 a sufficient fraction of the known $R_{1\rho}$ for 100 ppm Gd to give the best fit to a single BPP function together with a Korringa term. Best fits for the pure and purest $YH_{1.98}$ data were obtained using 16 and 2.5 ppm Gd, respectively, which is consistent with our knowledge of these specimens. The resulting parameters are the following: $\tau_0=2.0\times10^{-12}$ sec, $E_{\rm act}=435\pm5$ meV/atom, and $K=345\pm5$ sec K. The accuracy of τ_0 is difficult to decide but is probably not better than $\pm50\%$ if the uncertainty due to use of a BPP formula is included. The value of $E_{\rm act}$ agrees with that deduced directly from the slope of the $\log T_2$-vs-$10^3/T$ plot (Fig. 9) with no correction for residual impurity for the pure $YH_{1.98}$ specimen in the temperature range $2.1<10^3/T<2.8$ where T_2 is found to be insensitive to impurity. Confirmation of the $T_{1e}T$ value is obtained from further detailed treatment of the low-temperature data, discussed in Sec. VII.

The behavior of the $R_{1\rho}$ curves in the Gd-doped yttrium hydrides can be understood on the basis of the dipolar coupling of proton and impurity spins, combined with spin and particle diffusion,[47] using the theory outlined in Sec. II. The relevant length parameters β, b, and R, and the dimensionless ratio δ, have all been introduced there. To be specific, we consider the 100-ppm Gd sample. For this impurity concentration, $N=2.86\times10^{18}$ cm^{-3} and $R=44$ Å. Now the changeover from spin-diffusion to particle-diffusion dominance occurs when $D_a\approx D_s$, or equivalently when $\tau_D\approx T_2$. From the measured rigid-lattice $T_2=12$ μsec, we deduce that the changeover should occur at ~310 K, in satisfactory agreement with the temperature of the marked change in slope in Fig. 6.

As a representative value for the spin-diffusion regime we choose $R_{1\rho}=3.45$ sec^{-1}, observed at 40 MHz and 150 K for this specimen. At this temperature and frequency, $\omega_0^2\tau_i^2\approx0.004$ (with $\tau_iT=3.7\times10^{-8}$ sec K), showing that this is in the short-correlation-time regime for the major part of the dipolar coupling fluctuations, while the final term in Eq. (5) is negligible since $\omega_e^2\tau_i^2\gg1$. With $J=S=\frac{7}{2}$ and $g=2.0$ for the Gd^{3+} ion, Eq. (5) reduces to

$$C=1.55\times10^{-30}\tau_i\ , \tag{19}$$

so that at 150 K, $C=3.8\times10^{-40}$ sec^{-1}cm^{-6}. If we use the Lowe and Gade[30] result, the spin-diffusion coefficient $D_s=4.3\times10^{-12}$ cm^{2}sec^{-1}, and the pseudopotential radius $\beta=9.7$ Å. The spin-diffusion barrier radius b at the field $H_0=9395$ G corresponding to the proton resonance at 40 MHz is found from Eqs. (9) and (10) to be $b=9.7$ Å, and finally $\delta=0.50$. Thus the conditions $b,\beta<R$ are well

satisfied, and the situation is intermediate between the fast- and slow-diffusion regimes. The final result from Eq. (11) is $R_{1p}=4.1\ \text{sec}^{-1}$, in good agreement with the experimental value of 3.45 sec^{-1}, bearing in mind that no adjustable parameters have been employed so far but that a number of approximations have been made.

As can be seen in Fig. 6, R_{1p} increases slowly with decreasing temperature in the spin-diffusion regime below 250 K for all Gd concentrations. A temperature dependence is predicted by Eq. (11) since both β and δ vary with temperature because of their dependence on $B(x)$ [Eq. (10)] and on τ_i through the quantities C [Eq. (19)] and b [Eqs. (9) and (10)]. Again taking the 100-ppm Gd sample as representative and using the same parameter values as above, we find that Eq. (11) yields $R_{1p}\propto T^n$ with $n=-0.32$ compared with the experimental value of $n=-0.22$. In view of the approximations that have been made this measure of agreement is regarded as reasonably satisfactory.

Before turning to the atomic diffusion regime we consider the observed frequency dependence of T_{1p} at 200 K. Since $\omega_0^2\tau_i^2 \ll 1$ and $\omega_e^2\tau_i^2 \gg 1$, the frequency dependence cannot arise from these terms in the expression for C [Eq. (5)]. Moreover, there is no reason to suppose that τ_i is significantly field dependent, and hence frequency dependent, at this temperature. This leaves the field dependence of the diffusion barrier b, through Eqs. (9) and (10). Figure 16 shows the calculated frequency dependence from Eq. (11) using the same values of $\tau_i T$ and D_s as used above. For comparison, the slow-diffusion extreme given by Eq. (12) would yield no frequency dependence. The experimental points show a significant frequency dependence as expected if the situation lies between the slow and fast limiting regimes. In fact, the observed values are somewhat more frequency dependent than predicted. This in itself would suggest values of $\delta \lesssim 0.4$, compared with calculated values of 0.4—0.7, but this would be inconsistent with the absolute magnitudes of the observed T_{1p}. We are unable to account for this discrepancy in detail,

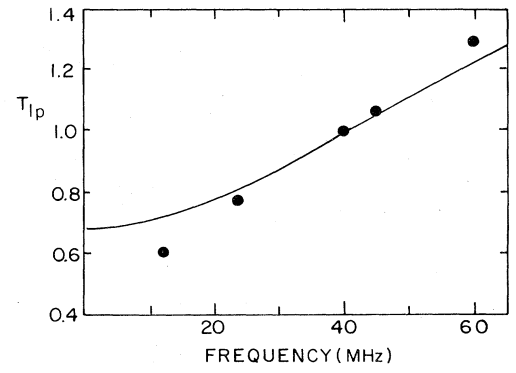

FIG. 16. Proton spin-lattice relaxation time due to Gd^{3+} in $YH_{1.99}$ + 475 ppm Gd at 200 K, measured as a function of frequency. The ordinate is T_{1p} normalized to the value at 40 MHz. The curve is the theoretical prediction without employing any adjustable parameters (see text).

but do not consider it serious in view of the approximations both in our model of $YH_{1.98}$(Gd), and in the use of a sharp diffusion cutoff at radius b.[32]

Above ~310 K, atomic diffusion becomes effective in transporting nuclear magnetization. Until the pseudopotential radius $\beta'=(C/D_a)^{1/4}$ becomes less than the shortest gadolinium ion-proton distance a_1, the relaxation is diffusion limited. For $YH_{1.98}$(Gd) the measured parameters yield a predicted temperature of ~400 K for the transition to the fast atomic diffusion, high-temperature regime. In the range 310—400 K, R_{1p} is seen to increase with increasing temperature (Fig. 6). The slopes of all the curves are the same and correspond to an activation energy of 0.29 eV/atom. The theory predicts that $R_{1p}\propto C^{1/4}D_a^{3/4}$; the temperature dependence is dominated by that of D_a and should display an apparent activation energy three-fourths of E_{act}, i.e., $\frac{3}{4}\times 0.435$ eV, which is satisfactorily close to the observed value.

Above 400 K where $\beta' < a_1$ Eq. (17) reduces to

$$R_{1p}=\tfrac{4}{3}\pi \text{Na}_1^3/\tau(a_1)\ ,$$

which can be written (in sec^{-1})

$$R_{1p}=1.62\times 10^{12}\left[\tau_i^*+\frac{7\tau_i^*}{3(1+\omega_e^2\tau_i^{*2})}\right]\ , \tag{20}$$

where $\tau_i^*\approx\tau_i$ since $\tau_i \ll \tau_D$ in the range of temperatures investigated. For temperatures greater than ~600 K the experimental data show no frequency dependence. This suggests that either $\omega_e\tau_i \gg 1$ or $\omega_e\tau_i \ll 1$, and that τ_i is field independent, which implies that there can be no appreciable contribution from phonon interactions to the electronic spin-lattice relaxation rate.

If the condition $\omega_e\tau_i \ll 1$ were satisfied at high temperatures, then the observed frequency dependence at lower temperatures (300 K $< T <$ 600 K) might be due to the $\omega_e\tau_i$ term, which will increase with decreasing temperature. Under that condition and assuming $\tau_i T=$const the slope of R_{1p} as a function of $1/T$ at 7 MHz for $T>600$ K may be fitted using $\tau_i T=1.1\times 10^{-8}$ sec K. This value of $\tau_i T$ is consistent with the analysis, since at $T=600$ K, $\tau_i\omega_e=0.5$, and hence could give rise to a frequency dependence but unfortunately yields values of R_{1p} at low temperatures in poor agreement with experiment. For example, for $T=150$ K, $R_{1p}=1.4\ \text{sec}^{-1}$ compared with the experimental value of 3.45 sec^{-1}.

On the other hand, if the alternative condition $\omega_e\tau_i \gg 1$ were satisfied at high temperatures the value of $\tau_i T$ deduced from the slope of the 7-MHz data would be 3.7×10^{-8} sec K in excellent agreement with the value deduced from ESR. However, in this case, no frequency dependence would be predicted at lower temperatures and the magnitude of the calculated value does not agree with experiment for $T>600$ K. We believe that the deviation in absolute value between theory and experiment at the highest temperatures is a result of extensive O-site occupation, as is planned to be discussed in a later publication.

Figure 17 compares the results of the entire calculation of R_{1p} on the basis of Eqs. (11) and (17) with the experimental data for the $YH_{1.98}$ + 100-ppm Gd sample mea-

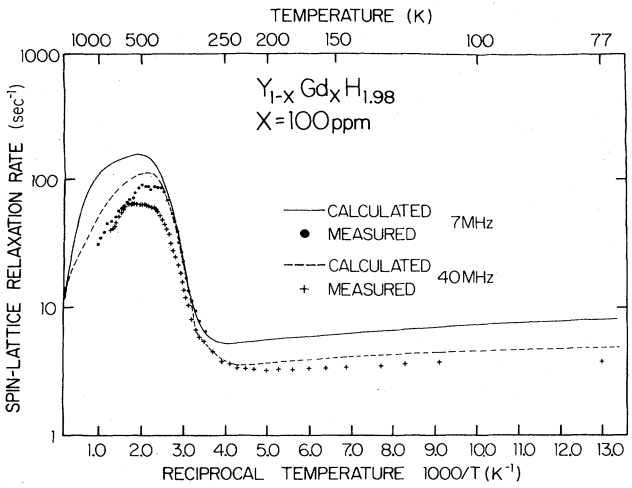

FIG. 17. Comparison of the experimental $R_{1\rho}$ values for $YH_{1.98}$ + 100 ppm Gd with the predictions of Eqs. (11) and (17). For the parameters used in these equations, see text.

sured at 7 and 40 MHz.

We now turn to the observations of T_2 shown in Figs. 8 and 9. We have already commented on the fact that T_2 falls below T_1 above $\sim$700 K even for the purest specimen and have associated this with a change of site occupation, to be discussed elsewhere. However, at temperatures between $\sim$550 and 700 K, T_1 and T_2 are equal to one another for all specimens and hence $T_{1\rho}$ and $T_{2\rho}$ are also equal. In fact, the data are entirely consistent with near equality of $T_{1\rho}$ and $T_{2\rho}$ throughout the temperature range investigated as expected from the considerations set out in Sec. II B 3. The absence of a detectable minimum in T_2 (as observed, for instance in the case[10] of PbF_2:Mn) is purely a question of the relative magnitudes of nuclear-nuclear and nuclear-impurity interactions. Similar considerations apply to $(T_{1\rho})_p$. In these materials no subsidiary minimum is observed in $T_{1\rho}$.[20] Around the main minimum of $T_{1\rho}$ and at lower temperatures the nuclear-nuclear dipolar contribution to $T_{1\rho}$ lies intermediate in value between T_1 and T_2. Since in this range, $T_{1\rho} \sim T_{2\rho} \sim (T_{1\rho})_p$, there is only a minor effect on the observed $T_{1\rho}$ values. (The observed asymmetry in the $T_{1\rho}$-T curve around the main minimum[20] is probably unrelated to impurity content and may result from diffusion in large background-field gradients present in the powder specimen, and possibly also partly from the severe experimental difficulties in keeping the amplitude of the rf field entirely constant as circuit parameters change with changing temperature.)

The data given in Fig. 3 show that for samples containing 20 ppm Gd, the subsidiary minimum in T_1 at 40 MHz moves to lower temperatures as the hydrogen content is increased, but the minimum becomes only slightly deeper. This behavior is consistent with our interpretation, which predicts that the minimum due to impurity relaxation will occur at the transition between the slow and fast atomic diffusion regions, that is when $\tau_D \sim \tau(a_1)$ the relaxation time for a proton fixed at the shortest gadolinium NN-proton distance a_1. The principal minimum in T_1 in Fig. 3 also shifts to lower temperatures with increasing hydrogen concentration, indicating that at a given temperature τ_D decreases as the hydrogen concentration increases. Since $\tau(a_1)$ is insensitive to temperature compared with τ_D, the above condition for the minimum due to impurity relaxation will be satisfied at progressively lower temperatures as the hydrogen content increases in qualitative agreement with experiment. As observed, the depth of the minimum is not expected to be particularly sensitive to hydrogen content although a small increase in the depth is predicted by Eq. (20) since the value of τ_i^* at the minimum increases as the latter moves to lower temperatures. Such behavior is just detectable in Fig. 3.

B. Effects of partial deuteration

We now consider the effects of partial deuteration in $La(H_{0.25}D_{0.75})_{2.25}$ shown in Fig. 14. We first consider the pure materials. The most obvious feature is the decrease in depth of the T_1 minimum, which is to be expected because the proton-proton dipolar contribution to the diffusion driven rate is reduced by a factor of 4, reasoning that deuterium substitutes randomly for hydrogen. Using a BPP model and allowing for the substantial ^{139}La-^{1}H interaction, as well as the small ^{2}D-^{1}H contribution in the deuterium-substituted sample, we estimate T_{1d} should be approximately 1.7 times larger at the minimum for the deuterated sample. After allowing for T_{1e}, the experimental factor is 1.9. Since the theoretical estimate is somewhat sensitive to the fractional O-site occupancy assumed and to any difference in τ_D values for deuterium and hydrogen (ignored in our estimate), the difference in these values will not be pursued. Indeed, the agreement is regarded as satisfactory for present purposes. (Of course, detailed measurements of such differences carry, in principle, information about isotopic differences in site occupancy and jump rates; such investigations are planned to be pursued elsewhere.)

To a good approximation no change in T_{1e} for the protons is expected on partial deuteration for a fixed combined H,D concentration. However, the observed T_1 is appreciably longer for the deuterated sample at low temperatures, and this difference is attributed to residual paramagnetic impurities. As already discussed, $T_{1\rho}$ in these samples at low temperatures depends upon D_s, i.e., we do not have the fast spin-diffusion limit. Since D_s is reduced by deuterium substitution, the residual $T_{1\rho}$ is also reduced. We therefore obtain the best estimate of T_{1e} from the deuterium substituted sample. This view is confirmed by the fact that, in this sample, T_1T is constant within experimental error ($T_1T = 442 \pm 3$ sec K) from 77 to 180 K, whereas in all other samples investigated the product decreases somewhat at temperatures below 180 K.

We now turn to the data shown in Fig. 14 for the Gd^{3+}-doped samples. At the main dipolar minimum the nuclear dipolar rate is reduced by the same amount (12 sec^{-1}) as that for the pure specimens, as expected. (In ar-

riving at this result the small difference in Gd^{3+} content between the two doped samples has been compensated). More interesting is the change in $T_{1\rho}$, where there is a clear difference in behavior between the atomic-diffusion- and spin-diffusion-dominated regions. This is shown more directly in Fig. 15 where $R_{1\rho}$, obtained by subtraction of the observed rates in the corresponding pure samples, is plotted as a function of reciprocal temperature. At temperatures above ~ 270 K there is very little difference between the data for the two samples other than that expected for slightly different Gd concentrations. In the slow atomic diffusion region, where $R_{1\rho}$ is changing rapidly with temperature, $R_{1\rho}$ would be marginally larger for the deuterated sample at equal Gd concentrations. This is most likely due to small differences in actual total H,D concentrations, but could possibly reflect a small decrease in τ_D for hydrogen on partial deuteration. But, essentially in agreement with theory, deuterium substitution has no significant effect on $R_{1\rho}$ since τ_D is very little affected, if at all.

For temperatures below ~ 270 K, on the other hand, deuteration causes a substantial reduction in $R_{1\rho}$, as predicted by Eq. (11), due to the reduction in D_s, for all except the fast-diffusion limit. In fact, one of the objectives of the deuterium substitution was to determine the values of δ appropriate to the specimens from the extent of the reduction. As discussed immediately, this has not proved possible. $R_{1\rho}$ is reduced by a factor of 2.8 at all temperatures between 110 and 180 K. This corresponds to a factor 2.55 between samples with precisely equal Gd concentrations. Equation (11) predicts a value lying between slightly less than unity (through b^3, in the fast-diffusion limit) and $(2.45)^{3/4}=1.96$ (through $D_s^{3/4}$, in the slow-diffusion limit). The latter factor allows for the effects of the unlike (La) nuclei on D_s as well as that of the changed hydrogen concentrations. Using best estimates of δ at 150 K, 0.67 and 0.97 for $LaH_{2.25}$ and $La(H_{0.25}D_{0.75})_{2.25}$, respectively, the theoretical ratio is about 1.5. The discrepancy is unlikely to be due to a change in τ_i on deuteration, and may indicate that, at low temperatures only (since $T_{1\rho}$ is unchanged by deuteration in the atomic diffusion regime) there is a preference for ^2D, rather than ^1H, to occupy sites nearest to Gd^{3+} ions.

C. Yttrium deuteride

Finally, we discuss the results for T_1 of deuterium nuclei in $YD_{1.88}$ shown in Fig. 10. In this system it is clear that the nuclear magnetic dipolar relaxation mechanism is not sufficiently strong to account for the results observed. In fact, if the T_1 minimum for $YH_{1.92}$ is scaled to allow for the difference between the magnetic moments of ^1H and ^2D, then the value of T_1 predicted at the minimum for ^2D is approximately 10 times the experimental value. Similarly, we expect the contribution to the rate from the conduction electrons T_{1e} to be very much smaller than for the corresponding hydride. The values of T_{1e} obtained by scaling the T_{1e} values for $YH_{1.92}$ by the ratio $\gamma^2(^2D)/\gamma^2(^1H)$ are shown in Fig. 10 for information.

It is generally found in metal-deuteride systems that the dominant contribution to the relaxation rate is due to the interaction between the electric quadrupole moment of the ^2D nucleus with randomly fluctuating electric field gradients, resulting from the diffusion of the deuterium atoms. Assuming that the quadrupolar relaxation rate may be described by the BPP model, we expect a maximum in the rate when $\omega_0\tau_D \sim 1$. More exact theories modify this result somewhat but the maximum still occurs near $\omega_0\tau_D \sim 1$. According to the classical picture in $YD_{1.88}$ τ_D will be given by

$$\tau_D = \sqrt{2}\tau_0 \exp(E_{\rm act}/k_B T)$$

and is thus increased by the factor $\sqrt{2}$ (the ratio of the square roots of the isotopic masses for ^2D and ^1H) over that for hydrogen but exhibits the same activation energy. As a result the minimum in the quadrupolar relaxation should be shifted by approximately 20 K relative to the position of the dipolar minimum in $YH_{1.92}$. As can be seen in Fig. 10, however, the minimum in $YD_{1.88}$ occurs at 411 K compared with 524 K for the dipolar minimum in $YH_{1.92}$, which is a much greater shift than predicted. Furthermore, the apparent activation energy deduced from the slope of T_1 vs $1/T$ on both sides of the minimum (assuming $T_1 \propto \omega_0^2\tau_D$ when $\omega_0\tau_D \gg 1$ and $T_1 \propto 1/\tau_D$ when $\omega_0\tau_D \ll 1$) is only 0.29 eV for $YD_{1.88}$ compared with 0.43 eV for $YH_{1.92}$. It therefore seems unlikely that the minimum in $YD_{1.88}$ is entirely due to quadrupole effects, and it seems probable that the presence of small amounts of Gd might be partly responsible for the results observed. The paramagnetic contribution to the ^2D relaxation rate has been calculated using Eq. (17). In the temperature range for which results have been obtained, atomic diffusion dominates since at the lowest temperature, $T=269$ K, $D_a = 4.6\times 10^{-11}$ cm^2 sec^{-1} compared with $D_s = 1.03\times 10^{-13}$ cm^2 sec^{-1} obtained using the Lowe and Gade result. In the calculation the values used for τ_D and τ_i are the same as those used in the earlier calculations for the hydrogen except that τ_D is increased by the $\sqrt{2}$ factor described above. It is assumed that the Gd concentration is 20 ppm, which is consistent with the known concentration of the pure yttrium dihydride samples. The results of the calculation are shown in Fig. 10 and show that even for the ^2D resonance, paramagnetic impurities can play an important role in relaxation, and indeed in this case, it appears that the impurity and quadrupole rates are quite comparable.

VI. TWO-SUBLATTICE MISINTERPRETATION OF THE T_1 MINIMA

As has already been remarked, the appearance of a subsidiary minimum on the low-temperature side of the principal T_1 minimum has been reported for a number of hydride systems including yttrium dihydride,[14] lanthanum dihydride,[48] and vanadium hydride.[49] This phenomenon has been interpreted in terms of hydrogen motion on two sublattices of interstitial sites, e.g., the T- and O-site sublattices. It is instructive to apply this type of analysis to the T_1 data for the $Y_{1-x}Gd_xH_{1.98}$ series of samples, since it will be seen that such a model can fit the data very well

and can therefore be extremely misleading.

Both NMR (Ref. 18) and neutron scattering[25] studies found premature occupancy of O-sites in yttrium dihydride. Therefore, a double BPP function formulation (sum of two single BPP functions) may be employed to interpret T_1 data showing double-minimum behavior. R_{1d} is taken to be the weighted sum of two functions of the form of Eq. (2), one representing the effect of T-T interactions and the second that of O-T interactions (that due to O-O interactions should be negligible). The assumption that the measured relaxation rate is the weighted sum of the rates for the two sublattices means that there exist a common spin temperature and a single T_1 for all protons on both sublattices. This is consistent with the fact that in all these measurements only exponential magnetization recoveries and single T_1's were observed. This is certainly reasonable since the T- and O-site sublattices are in fact interpenetrating so that the NN of each species are on the other sublattice.

Examples of such fits to the measured T_1 data for the nominally pure and purest $YH_{1.98}$ samples at 40 MHz are shown in Fig. 18. These fits include a Korringa term but not an impurity-induced contribution. The fit to the data is rather good over the whole temperature range for the 2-ppm Gd sample, and the inadequacy of this analysis is only shown up for the 20 ppm Gd sample by the lowest temperature observations.

The deceiving character of the impurity-induced subsidiary minimum is further demonstrated by the fact that the values of O-site occupancy deduced from the T_1 data for the set of pure yttrium dihydrides shown in Fig. 3 are, quite accidentally as we know, in good agreement with the values which had been determined by both NMR (Ref. 18) and neutron scattering measurements.[25] In the two-sublattice model, the ratio of the maximum relaxation rates $R_{1T,\max}$ and $R_{1O,\max}$ is related to the ratio of hydrogen occupancies in the T and O sites but weighted by the ratio of the dipolar second moments associated with T-T and O-T interactions. The results of fitting the two-sublattice model to the data of Fig. 3 (of which Fig. 18 furnishes an example) are that approximately 7—13 % of octahedral sites are occupied in the temperature region around the T_1 minima, with little change between the samples with $x=1.91$ and 2.03. These values are similar to those previously reported,[18,25] although the substantial increase in O-site occupancy between $x=1.9$ and 2.0 shown by the wide-line NMR (Ref. 18) is not reproduced.

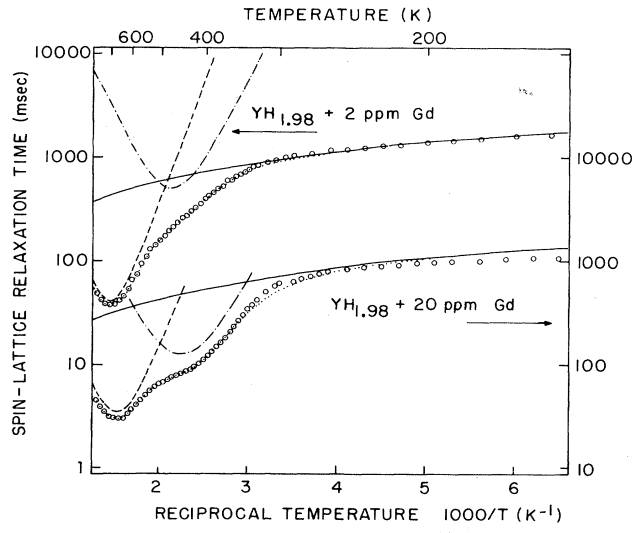

FIG. 18. Comparison of T_1 data for pure (20 ppm Gd) and purest (2 ppm Gd) $YH_{1.98}$ samples at 40 MHz. As can be seen, double BPP functions may be fit to each data set rather well.

To summarize, the appearance of the subsidiary minimum depends on Gd concentration in the samples investigated. Similar results have been obtained for scandium and lutetium hydrides, and as will be shown[26] other rare-earth impurities in the yttrium and lanthanum hydrides also give rise to subsidiary minima and slope-change effects that depend on both the particular ion and its concentration. Misinterpretation of all these effects in terms of two types of hydrogen motion can readily occur.

VII. DIFFICULTY OF DETERMINING THE KORRINGA PRODUCT

As has been demonstrated in Secs. IV and V, in the rigid-lattice regime the impurity-induced relaxation rate resulting from spin diffusion to the paramagnetic centers can contribute strongly to the total measured rate even for very low impurity levels. This makes it difficult to extract unambiguously the conduction-electron contribution R_{1e} and therefore the Korringa product, which is of particular interest since $(T_{1e}T)^{-1/2}$ is considered to be proportional to the density of states at the Fermi level $N(E_F)$.[50] In this section we focus on the low-temperature behavior of T_1 and on the difficulties involved in correctly partitioning R_1 between R_{1e} and R_{1p}.

For high impurity levels (of the order of 500 ppm or greater in this study) the measured T_1 in the rigid-lattice regime clearly passes through a maximum with decreasing temperature and then decreases with further decreasing temperature (at least down to 77 K). This behavior is shown schematically in Fig. 1, and examples may be found in Refs. 5, 14, 26, and 48 for example. In such cases meaningful separation of R_{1e} and R_{1p} cannot be made.

A more dangerous situation arises in the case of "nominally pure" samples (impurity content of the order of 20 ppm or less in this study). Then the presence of the impurity contribution is not as obvious. We consider the measurements on the pure and purest yttrium dihydrides presented in Sec. IV to be illustrative. As seen in Fig. 3 the values of T_1 in the rigid-lattice regime for all the pure YH_x samples increase very slowly with decreasing temperature. This is even more apparent in Fig. 4, which compares the pure and purest $YH_{1.98}$ samples, the data shown being extended to lower temperatures than in Fig. 3. T_1 continues to increase with decreasing temperature down to 77 K, the lowest temperature at which measurements were made. On the other hand, the value of the

product T_1T, formed from the measured T_1's, passes through a maximum with decreasing temperature. This is illustrated in Fig. 19 for the data of Fig. 4. The maximum is a consequence of the interplay of the three contributions to T_1T, namely, $T_{1e}T$, which is expected to be constant, $T_{1d}T$, which increases rapidly with decreasing temperature as T_{1d} becomes very large, and $T_{1p}T$, which decreases relatively slowly depending on the ion species and concentration.

One method that may be used to analyze the T_1T data for the two samples shown in Fig. 19 for the temperature region below the maximum T_1T (i.e., in the temperature range in which T_{1d} is no longer significant) in order to yield the Korringa product and R_{1p} and its temperature dependence is the following. We assume that $T_{1e}T$ is independent of impurity concentration, at least for low concentrations, and that $T_{1p}=cT^n$ where n is a constant to be determined. The latter should be a good approximation provided that we do not reach so low a temperature such that $\omega_0\tau_i\sim 1$. It is not necessary that the impurity concentration be known. Taking data for any two temperatures in this range for the two samples, we can solve for the four unknowns $T_{1e}T$, c_1, c_2 and n. For the data of Fig. 19 we thus obtain $K=346$ sec K. This value is substantially greater than the maximum T_1T product (305 sec K), as seen in Fig. 19.

This result may be compared with that of another method that has been used[51,52] to determine K, which involves plotting the total relaxation rate R_1 in the rigid-lattice regime versus temperature. Since in this case, $R_1=R_{1e}+R_{1p}$, then assuming that R_{1p} is *constant* and independent of temperature, such a graph should yield a straight line whose slope gives the Korringa product and whose intercept on the R_1 axis gives the (constant) impurity rate R_{1p}. We have applied this method of analysis to the data for three of the $YH_{1.98}$ samples, those with 2, 20, and 50 ppm Gd (i.e., the two samples discussed above plus the 50-ppm Gd sample). The resulting graphs are shown in Fig. 20 where the solid lines are least-squares fits to the "straight-line" portions of the data in each case. It is clearly evident in the case of the 50-ppm sample that R_1 passes through a minimum in the vicinity of 100 K, so that this straight-line region is somewhat arbitrary. Similar behavior is just apparent in the data for the 20-ppm sample. The K values obtained from the slopes of the lines increase with increasing impurity content. However, the value obtained for the purest sample, $K=349$ sec K, is in excellent agreement with that derived above (346 sec K). This exercise demonstrates that the method of analysis illustrated in Fig. 20, which assumes that T_{1p} is a temperature-independent constant, can yield the true Korringa product only if the impurity concentration is sufficiently low. The method is clearly not appropriate when R_1 itself passes through a minimum, as in the case of the 50-ppm Gd sample in Fig. 20. (See, also, Ref. 51.)

To summarize, the two methods of analysis that we have outlined enable one to obtain the true Korringa product if (a) the impurity content is sufficiently low so that T_{1p} can be approximated to be temperature independent (Fig. 20), or (b) if T_1T data for two (or more) levels of impurity concentration are available, even if the concentrations are not known (analysis of Fig. 19). As demonstrated, the two methods yield the same result. The maximum value of T_1T itself is always less than the true $T_{1e}T$. In the present case, even for the purest sample, the maximum T_1T is 87% of $T_{1e}T$. A further method exploits the fact that T_{1p} is in general, frequency dependent and can be removed by extrapolation to infinite frequency. We plan to utilize this method in a forthcoming study of lanthanum trihydride. Finally, as we have shown, partial deuteration

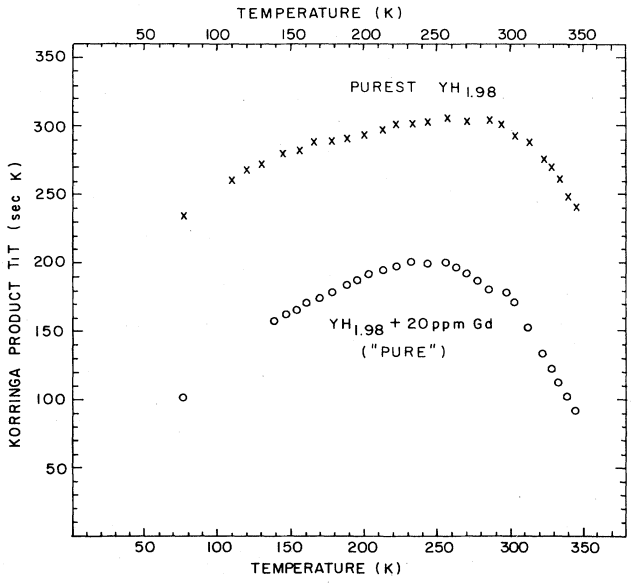

FIG. 19. Comparison of the T_1T products taken from the 40-MHz data obtained for the pure and purest samples of $YH_{1.98}$, showing that T_1T passes through a maximum as a function of temperature.

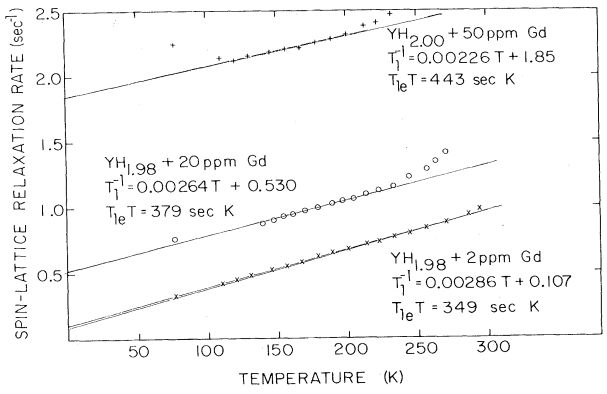

FIG. 20. Temperature dependence of the measured proton spin-lattice relaxation rate R_1 in $YH_{1.98}$ at low temperatures measured at 40 MHz for the three samples with lowest Gd contents. The solid lines are least-squares fits to the straight-line portions of the data in each case. The resulting fit parameters are shown on the figure.

can be a powerful tool in separating the various components of spin-lattice relaxation.

VIII. CONCLUSIONS

The primary contribution that this investigation has made to the utilization of NMR in studies of metal hydrides has been the clear demonstration that the presence of paramagnetic impurity ions in concentrations so low as to have heretofore been regarded as insignificant can have marked effects on the temperature dependence of the proton relaxation times as well as on electronic structure and hydrogen diffusion parameters derived from such measurements. Paramagnetic ions contribute an additional relaxation process, which in the yttrium and lanthanum dihydrides appears to be entirely due to the dipolar coupling between impurity and proton moments. Protons close to the impurity ions are directly relaxed. At low temperatures, protons far from the impurity ions (relaxation centers) are relaxed by the mechanism of spin diffusion. For Gd^{3+} ions in YH_x and LaH_x, the temperature and field dependences of the proton T_1 indicate that such relaxation by spin diffusion is intermediate between the slow and fast regimes of spin diffusion. At higher intermediate temperatures, hydrogen-atom diffusion becomes more rapid than spin diffusion and takes over as the mechanism for transporting distant spin magnetization to the relaxation center. This process is (atom) diffusion limited, and since atom diffusion increases greatly with increasing temperature, relaxation in the intermediate region reaches rates 20—25 times faster than those at low temperatures. At still higher temperatures, hydrogen diffusion becomes so rapid that the duration of individual encounters with impurity moments becomes too short for relaxation to occur efficiently. This is the fast- (atom) diffusion regime, and the relaxation rate passes through a broad maximum and then decreases slowly with further increasing temperature.

This behavior has been most clearly documented in this study for the Gd^{3+} ion introduced into both $YH_{1.98}$ and $LaH_{2.25}$ at controlled levels as low as 50 ppm atomic concentration. Effects were also unambiguously observed in samples containing uncontrolled levels of paramagnetic impurities as low as 2—5 ppm.

As remarked above, the impurity-induced relaxation makes it very difficult to extract unambiguously the NMR parameters characterizing the electronic structure (the Korringa product $K = T_{1e}T$) and hydrogen diffusion (jump frequency and activation energy). Regarding determinations of K, it has been almost invariably assumed heretofore that at low temperatures the impurity-induced rate $R_{1\rho}$ is temperature independent, and that it can be estimated by appropriate extrapolations of data from restricted temperature ranges. Yet the measurements made in this study show that *in every system investigated,* $R_{1\rho}$ is temperature dependent, in some cases quite strongly. Even the purest samples showed evidence of departure from ideal Korringa behavior at low temperatures consistent with relaxation by paramagnetic impurities.

To counter these difficulties, several procedures are suggested and demonstrated for obtaining the true Korringa product values. Of these methods, the most unambiguous is that of partial deuteration of the hydride, thereby reducing substantially the spin-diffusion rate of protons and hence $R_{1\rho}$. This procedure can be followed without knowing the impurity content of the hydride sample. Other procedures require knowledge of the frequency dependence of T_1, or of the impurity content or the availability of samples with different levels of impurity (but not necessarily known).

TABLE III. Spark-source mass-spectrometric analysis (atomic ppm) for Ames Laboratory yttrium, Y-12979-W, which was used to prepare the series of yttrium dihydrides YH_x, $1.81 \leq x \leq 2.03$. Semiquantitative survey of the rare-earth impurities. Also given are vacuum fusion results; wt. ppm in parentheses.

Li	0.005	Be	<0.002	B	<0.08	Na	<0.1	Mg	<0.04	Al	6	Si	1	F	<0.05
S	0.5	Cl	2	K	<0.09	Ca	0.10	Ti	2.1	V	<0.2	Cr	1	Mn	0.10
Fe	15	Co	<0.2	Ni	2	Cu	4	Zn	0.29	Ga	<0.05	Ge	<0.05	As	<0.01
Se	<0.1	Br	<0.04	Rb	<0.009	Sr	<1	Zr	<2	Nb	<0.1	Mo	<0.5	Ru	<0.6
Rh	<0.3	Pd	<1	Ag	<0.03	Cd	<0.06	In	<0.03	Sn	0.70	Sb	<0.04	Te	<0.05
I	<0.04	Cs	<0.003	Ba	<0.07	Hf	<2	Ta	2	W	40	Re	<0.3	Os	<0.5
Ir	<0.2	Pt	<0.3	Au	<0.05	Hg	<0.06	Tl	<0.04	Fb	1	Bi	<0.03	Th	<0.4
														U	<0.2
							Rare-earth impurities								
Sc	<0.1	Y		La	1.5	Ce	2.4	Pr	0.52	Nd	<0.5	Sm	<0.3	Eu	<0.1
Gd	<20	Tb	1	Dy	<0.6	Ho	<0.1	Er	<0.4	Tm	<0.1	Yb	<4	Lu	2
							Vacuum fusion results								
O	411 (74)			N	25 (4)			H	880 (10)						
	Combustion								Absorption						
C	282 (38)							F	98 (21)			Fe		17 (11)	

TABLE IV. Spark-source mass-spectrometric analysis (atomic ppm) for Ames Laboratory yttrium, Y-12381B, which was used to prepare the purest $YH_{1.98}$ and the series of Gd-doped samples, $Y_{1-x}Gd_xH_{1.98}$. Semiquantitative survey for the rare-earth impurities. Also given are vacuum fusion results; wt. ppm in parentheses.

Li	<0.000	Be	<0.002	B	0.07	Na	<0.1	Mg	0.10	Al	3	Si	3	P	<0.03
S	<0.1	Cl	3	K	<0.04	Ca	0.10	Ti	0.80	V	<0.03	Cr	0.5	Mn	<0.04
Fe	10	Co	<0.05	Ni	3	Cu	5	Zn	<0.06	Ga	<0.06	Ge	<0.08	As	<0.02
Se	<0.1	Br	<0.05	Rb	<2000	Sr	<0.1	Zr	<0.3	Nb	<0.8	Mo	<0.8	Ru	<0.6
Rh	<0.1	Pd	<0.3	Ag	<0.04	Cd	<0.08	In	<0.03	Sn	<0.1	Sb	<0.05	Te	<0.06
I	<0.04	Cs	<0.004	Ba	<0.08	Hf	<0.8	Ta	<0.6	W	20	Re	<0.4	Os	<0.2
Ir	<0.09	Pt	<0.3	Au	<0.07	Hg	<0.08	Tl	<0.06	Pb	20	Bi	<0.04	Th	<0.5
														U	<0.2
							Rare-earth impurities								
Sc	<1	Y		La	3	Ce	2	Pr	4.0	Nd	<0.6	Sm	<0.4	Eu	<0.2
Gd	2.1	Tb	4.5	Dy	<0.4	Ho	<0.2	Er	<0.5	Tm	<0.1	Yb	<0.3	Lu	<0.3
							Vacuum fusion results								
O		834 (150)		N		25 (4)		H		704 (8)					
		Combustion								Absorption					
C		141 (19)						F		<14 (<3)		Fe		8 (4.9)	

The impurity-induced relaxation has also been shown to have profound effects on the apparent nuclear-nuclear dipolar relaxation rate. At impurity levels as low as 10 ppm in the case of Gd^{3+}, a secondary minimum in the temperature dependence of the proton T_1 appears, which may be readily misinterpreted in terms of a second motional process of the diffusing hydrogen. Even lower impurity levels yield a characteristic "slope change" on the low-temperature side of the principal T_1 minimum. This slope change may be erroneously interpreted in terms of a change in activation energy for diffusion. The results obtained in this investigation strongly suggest that in a truly impurity-free metal hydride, only a single minimum in the temperature dependence of the proton T_{1d} would be obtained without any indication of a secondary minimum or charge in slope on the low-temperature side of the minimum.

In summary, we have shown that the interpretation of "anomalous" temperature-dependent behavior of proton T_{1d} in metal hydrides in terms of changes and/or unusual character of the hydrogen diffusion process must be regarded with caution until it can be demonstrated that

TABLE V. Spark-source mass-spectrometric analysis (atomic ppm) for Ames Laboratory lanthanum, La-8681, which was used to prepare pure $LaH_{2.27}$ and the series of Gd-doped samples, $La_{1-x}Gd_xH_{2.25}$. Semiquantitative survey for the rare-earth impurities. Also given are vacuum fusion results; wt. ppm in parentheses.

Li	0.005	Be	<0.001	B	<0.2	Na	<1	Mg	<0.05	Al	5	Si	30	P	0.08
S	<0.5	Cl	4	K	<0.3	Ca	<0.4	Ti	0.21	V	0.66	Cr	<0.03	Mn	<0.02
Fe	2	Co	<0.06	Ni	2.8	Cu	<0.06	Zn	<0.03	Ga	<0.1	Ge	<0.06	As	<0.2
Se	<0.04	Br	<0.03	Rb	<0.006	Sr	<0.02	Zr	<0.2	Nb	<2	Mo	<0.4	Ru	<0.06
Rh	<0.06	Pd	<0.1	Ag	<0.02	Cd	<0.05	In	<0.03	Sn	<0.08	Sb	<0.03	Te	<0.05
I	<0.03	Cs	<0.1	Ba	<0.8	Hf	<0.7	Ta	1.9	W	<1	Re	<0.4	Os	<0.5
Ir	<0.2	Pt	0.31	Au	<0.06	Hg	0.20	Tl	<0.04	Pb	0.20	Bi	<0.03	Th	<0.4
														U	<0.2
							Rare-earth impurities								
Sc	<0.02	Y	3.1	La		Ce	4	Pr	1	Nd	<1	Sm	<0.4	Eu	<0.2
Gd	<0.5	Tb	<0.1	Dy	<0.5	Ho	<0.2	Er	<0.5	Tm	<0.1	Yb	<0.2	Lu	<0.3
							Vacuum fusion results								
O		243 (28)		N		59 (6)		H		137 (1)					
		Combustion								Absorption					
C		23 (2)						F		65 (9)		Fe		9 (3.7)	

these effects are not the consequence of paramagnetic impurities. Since T_2 and $T_{1\rho}$ may be much less influenced by impurities in at least part of the relevant temperature range, they may be preferable to T_1 as tools for studying the diffusion. Likewise, Korringa product estimates can easily err significantly if the paramagnetic impurity-induced rate $R_{1\rho}$ is treated as temperature independent. Much greater attention to both the control and characterization of the paramagnetic impurity content of metal hydrides for NMR studies is essential. Finally, these effects must at present be regarded as a severe nuisance. However, it seems likely that, once they are thoroughly understood, they may be found to be useful as an additional method of exploring the microscopic behavior of dissolved hydrogen. We are taking initial steps in this direction with a study of hydrogen trapping around substitutional (paramagnetic) ions in a variety of metal hydrides.

ACKNOWLEDGMENTS

The support provided by a grant from the North Atlantic Treaty Organization Grant No. 071-80 is gratefully acknowledged by both research groups (Ames Laboratory and University of Warwick). One of us (E.F.W.S.) expresses his appreciation for the hospitality of the Ames Laboratory, where part of this work was completed. The authors are indebted to Dr. R. J. Schoenberger for assistance with the calculation aspects of this work and to Mr. A. Johnson for his careful preparation of the hydride samples for NMR study. Ames Laboratory is operated for the U.S. Department of Energy by Iowa State University under Contract No. W-7405-Eng-82. This work was supported by the Director for Energy Research, Office of Basic Energy Sciences. The work at Cornell University was supported in part by National Science Foundation Grant No. DMR-79-25373. The work at the University of Warwick was supported by the United Kingdom Science and Engineering Research Council.

APPENDIX

We list here in Tables III—V the spark-source mass-spectrometric analyses of the several different batches of lanthanum and yttrium metals that were used in the preparation of the hydrides studied in this invesgitation. All of the analyses were made in the Analytical Services Department of the Ames Laboratory.

[1]R. M. Cotts, Ber. Bunsenges. Phys. Chem. 76, 760 (1972).
[2]R. M. Cotts, in *Hydrogen in Metals I, Basic Properties,* edited by G. Alefeld and J. Völkl (Springer, Berlin, 1978).
[3]R. M. Cotts, in *Proceedings of the International Symposium on the Electronic Structure and Properties of Hydrogen in Metals, 1982, Richmond, Virginia,* edited by P. Jena and C. Satterthwaite (Plenum, New York, 1983).
[4]J. Korringa, Physica (Utrecht) 16, 601 (1950).
[5]D. S. Schreiber and R. M. Cotts, Phys. Rev. 131, 1118 (1963).
[6]S. M. Day, E. Otsuka, and B. Josephson, Jr., Phys. Rev. 137, A108 (1965).
[7]T. L. Guzzle and P. P. Mahendroo, Phys. Rev. 150, 361 (1966).
[8]F. Y. Fradin, Phys. Rev. Lett. 26, 1033 (1971); P. Bernier and H. Alloul, J. Phys. F 3, 869 (1973).
[9]L. Shen, Phys. Rev. 172, 259 (1968).
[10]S. P. Vernon, P. Thayamballi, R. D. Hogg, D. Hone, and V. Jaccarino, Phys. Rev. B 24, 3756 (1981).
[11]A. Abragam, *The Principles of Nuclear Magnetism* (Clarendon, Oxford, 1961), p. 328.
[12]C. A. Sholl, J. Phys. C 14, 447 (1981).
[13]H. T. Weaver, Phys. Rev. B 5, 1663 (1972).
[14]R. S. Kashaev, E. F. Gubaidullin, A. N. Gil'manov, and M. E. Kost, Fiz. Tverd. Tela (Leningrad) 22, 906 (1980) [Sov. Phys.—Solid State 22, 530 (1980)].
[15]T. C. Jones, T. K. Halstead, and K. H. J. Buschow, J. Less-Common Met. 73, 209 (1980).
[16]D. L. Anderson, R. G. Barnes, S. O. Nelson, and D. R. Torgeson, Phys. Lett. 74A, 427 (1979).
[17]D. G. de Groot, R. G. Barnes, B. J. Beaudry, and D. R. Torgeson, Z. Phys. Chem. N. F. 114, 83 (1979).
[18]D. L. Anderson, R. G. Barnes, D. T. Peterson, and D. R. Torgeson, Phys. Rev. B 21, 2625 (1980).
[19]D. G. de Groot, R. G. Barnes, B. J. Beaudry, and D. R. Torgeson, J. Less-Common Met. 73, 233 (1980).
[20]D. L. Anderson, T. Y. Hwang, R. G. Barnes, D. T. Peterson, and D. R. Torgeson, J. Less-Common Met. 73, 243 (1980).
[21]R. G. Barnes, B. J. Beaudry, R. B. Creel, D. R. Torgeson, and D. G. de Groot, Solid State Commun. 36, 105 (1980).
[22]F. Borsa, R. G. Barnes, D. R. Torgeson, and B. J. Beaudry, Phys. Rev. B 26, 1471 (1982).
[23]W. M. Mueller, J. P. Blackledge, and G. G. Libowitz, *Metal Hydrides* (Academic, New York, 1968), p. 443.
[24]R. N. Shelton, P. Klavins, R. G. Barnes, and B. J. Beaudry, Bull. Am. Phys. Soc. 27, 224 (1982).
[25]D. Khatamian, W. A. Kamitakahara, R. G. Barnes, and D. T. Peterson, Phys. Rev. B 21, 2622 (1980).
[26]T. T. Phua *et al.* (unpublished).
[27]N. Bloembergen, E. M. Purcell, and R. V. Pound, Phys. Rev. 73, 679 (1948) (referred to as BPP).
[28]H. G. Bohn and R. R. Arons, J. Appl. Phys. 53, 2072 (1982).
[29]H. E. Rorschach, Jr., Physica (Utrecht) 30, 38 (1964).
[30]N. Bloembergen, Physica (Utrecht) 25, 386 (1949).
[31]I. J. Lowe and S. Gade, Phys. Rev. 156, 817 (1967).
[32]E. P. Horvitz, Phys. Rev. B 3, 2868 (1971).
[33]G. R. Khutsishvili, Zh. Eksp. Teor. Fiz. 42, 1311 (1962) [Sov. Phys.—JETP 15, 909 (1962)].
[34]P. G. de Gennes, Phys. Chem. Solids 7, 345 (1958).
[35]P. M. Richards, Phys. Rev. B 25, 1514 (1982).
[36]W. Blumberg, Phys. Rev. 119, 79 (1960).
[37]P. M. Richards, Phys. Rev. B 18, 6358 (1978).

[38]I. J. Lowe and D. Tse, Phys. Rev. 166, 279 (1968).
[39]I. J. Lowe and C. E. Tarr, J. Phys. E 1, 320 (1968).
[40]J. L. Conway and R. M. Cotts, Rev. Sci. Instrum. 48, 636 (1977).
[41]D. J. Adduci, P. A. Hornung, and D. R. Torgeson, Rev. Sci. Instrum. 48, 661 (1977).
[42]D. J. Adduci, P. A. Hornung, and D. R. Torgeson, Rev. Sci. Instrum. 47, 1503 (1976).
[43]D. R. Torgeson (unpublished).
[44]DATA routine of BIONIC program, R. G. Lecander and D. R. Torgeson (unpublished).
[45]D. J. Adduci and D. R. Torgeson (unpublished).
[46]H. Drulis, Arch. Sci. (Geneva) 27, 243 (1974).
[47]M. Belhoul, G. A. Styles, E. F. W. Seymour, T.-T. Phua, R. G. Barnes, D. R. Torgeson, and D. T. Peterson, J. Phys. F 12, 2455 (1982).
[48]R. S. Kashaev, A. N. Gil'manov, F. F. Gubaidullin, and M. E. Kost, Fiz. Tverd. Tela (Leningrad) 20, 3 (1978) [Sov. Phys.—Solid State 20, 1 (1978)].
[49]Y. Fukai and S. Kazama, Acta Metall. 25, 59 (1977).
[50]See for example, A. Narath, in *Hyperfine Interactions,* edited by A. J. Freeman and R. B. Frankel (Academic, New York, 1967).
[51]O. J. Zogal and S. Idziak, Physica (Utrecht) 104B, 365 (1981).
[52]R. Göring, R. Lukas, and K. Bohmhammel, J. Phys. C 14, 5675 (1981).